Optimization of normal phase chromatographic conditions for lipid analysis and comparison of associated detection techniques

Sonia Abreu, Audrey Solgadi, Pierre Chaminade

DOI 10.1016/j.chroma.2017.07.063

Optimization of normal phase chromatographic conditions for lipid analysis and comparison of associated detection techniques

Sonia Abreu [a], Audrey Solgadi[b], Pierre Chaminade [a,*]

[a] Lip(Sys)-², Chimie Analytique Pharmaceutique (FKA EA4041 Groupe de Chimie Analytique de Paris-Sud), Univ. Paris-Sud, Université Paris-Saclay, F-92290 Châtenay-Malabry, France.
[b] SAMM, UMS IPSIT, Université Paris Sud, Université Paris-Saclay, Chatenay-Malabry, France

[*]Corresponding author. Tel: +3346835459; Fax: +3346835458
E-mail address: pierre.chaminade@u-psud.fr

Abstract

One important challenge in lipid class analysis is to develop a method suitable or, at least adaptable, for a vast diversity of samples. In the current study, an improved normal-phase liquid chromatography (NPLC) method allowed analyzing the lipid classes present in mammalian, vegetable as well as microorganism (yeast and bacteria) lipid samples. The method effectively separated 30 lipid classes or subclasses with a special focus on medium polarity lipids. The separation was carried out with bare silica stationary phase and was coupled to evaporative light scattering detection (ELSD), charged aerosol detection (Corona-CAD®) and mass spectrometry. Solutions are provided to circumvent technical issues (such as pumping solvents of low viscosity, solvent purity, rinsing step). The influence of mobile phase composition and addition of ionic modifiers on the chromatographic behavior of particular lipid classes is documented. A comparison between ELSD and Corona-CAD® confirmed the interest of this later detector for samples with a wide range of concentration of different lipids. Three common atmospheric pressure ionization interfaces were used for coupling the NPLC separation to a LTQ Velos Pro® mass spectrometer. The comparison of the chromatographic profiles showed that atmospheric pressure chemical ionization (APCI) and atmospheric pressure photoionization (APPI) are both suitable to detect the different lipid classes whereas APPI allows a better sensitivity for lipids at low-concentration.

Keywords:

Lipids

Normal-phase liquid chromatography

Evaporative Light Scattering Detector

Charged Aerosol Detector

Atmospheric pressure photoionization

LC/MS

1. Introduction

Lipidomics has emerged with the growing progress in mass spectrometry and bioinformatics. This is a complex field of activity since more than 40 000 unique lipid structures are listed in the LIPIDMAPS database nowadays [1,2]. Analytical techniques for lipidomics represent a very dynamic and motivating area as the lipid composition of animal or vegetal tissue is influenced by external factors (such as metabolic state or diet) and as research methods have still to be developed. New technologies and/or new developments in analytical sciences are now addressing lipid analysis to promote alternative and original separation techniques coupled with mass spectrometry. An important review about LC/MS based lipid analysis was published by Cajka & Fiehn [3] in 2014. They analyzed 185 original research papers and covered the technical approaches involved in lipidomics. The scope ranges from sample preparation to data treatment and encompasses mass spectrometry and separation techniques.

Several interesting findings can be extracted from this article. First, the diversity of the biological samples addressed by these 185 studies: plasma and serum represent 39% of the samples, animal tissue 23% and cells 22%, only 3% are plant tissues and other matrix represent 13%. Second, when LC/MS is used, reversed-phase liquid chromatography (RPLC), normal phase liquid chromatography (NPLC) and hydrophilic interaction chromatography (HILIC) are the most important techniques and correspond respectively to 71, 19 and 8% of the studies. It is worthy to note that RPLC and HILIC take advantage of improved sub-2-µm or fused core 2.6-2.8µm particle size stationary phases whereas NPLC methods use classical 3-5µm. In the vast majority of cases, narrow bore columns (2.1 mm I.D.) are used whatever is the retention mechanism. RPLC and HILC benefit from the high water content and water miscible solvents used as mobile phase that facilitate the coupling with MS. HILIC is presented as an alternative to NPLC with a better reproducibility and a better compatibility with MS. Finally, this review pointed out the dominant position of electrospray ionization mass spectrometry (ESI) in lipidomic studies, most of time used in positive mode. At the opposite, atmospheric pressure chemical ionization (APCI) appears to be limited to nonpolar lipids (mainly triacylglycerols).

With regard to separation techniques, the recent trends in lipidomic analysis can be illustrated by four impressive studies issued by Holčapek's group. Two of them concern alternative retention mechanisms (namely HILIC) or separation techniques i.e. supercritical fluid chromatography (SFC) and their coupling to MS. The two remaining studies take advantage of multidimensional techniques such as LCxLC or LCxIon Mobility to deal with sample complexity.

In a recent work (2016) [4], a considerable effort was made to optimize the HILIC separation of acidic phospholipids. This separation appears to be also suitable for medium polarity lipids (such as ceramides)

but, in case of a total lipid extract, both NPLC and HILIC must be employed to accommodate the sample complexity and polarity [5]. The most nonpolar lipids cannot be retained in HILIC conditions.

SFC offers both efficiency and analysis speed when used with modern sub 2µm particles. A high-throughput method by UHPSFC coupled with electrospray ionization mass spectrometry (ESI-MS) with a chromatography column packed with silica particles of less than 2 µm (2015) [6] was proposed. 24 classes of lipids were separated in 6 min and 436 lipid species were identified in a porcine brain extract. The CO_2 co-solvents used were only water and methanol.

When the lipid sample is extremely complex, one-dimensional analysis becomes insufficient. The second trend is to enhance the discriminating power of the chromatographic system by adding a supplementary separation step before the mass spectrometer entry. Two-dimensional liquid chromatography-electrospray ionization mass spectrometry (2D LCxLC ESI-MS) was developed for the comprehensive and simultaneous separation of classes and species of lipids (2015) [7]. The authors used RPLC with a C18 column in the first dimension (150 min), and HILIC with a silica column in the second dimension (1 min). Finally, in a study dealing with the complex analysis of the regioisomers of triacylglycerol by differential mobility ESI-MS (2016) [8], the authors describe how ionic mobility permits the separation of compounds which are chromatographically co-eluted.

All these recent studies take advantage of recent sub 2µm or fused core particles that allow fast and efficient separations. This trend is only scarcely represented when considering normal phase separations. In 2011, McLaren [9], adapted the separation of total lipids to a Fused-Core particle column using UHPLC. He used an Halo HILIC column with 2.7 µm particle, but carried out the separation in normal-phase mode with evaporative light scattering detection (ELSD). The separation of the main lipids found in plasma, liver and heart was realized in 10 min. The method was developed with only 7 different lipid standards; however it is advisable form the chromatogram that more lipid classes could be separated using this method. The solvent program appears to be very similar to the one proposed by Christie [10] for mammalian lipid class analysis .

Thus, despite of its typically longer analysis time, NPLC remains attractive for the analysis of a total lipid extract and the objective of a complete separation of lipid classes. Method development is more complex in NPLC than in RPLC. The mobile phases are usually made of solvent mixtures to ensure miscibility and to encompass a wide range of polarity. The main advantage of NPLC is the elution of lipids according to their polar moieties or “head group” which also define their family or “lipid class”. Even complex lipid mixtures lead to easily interpretable chromatograms where molecular species of the same class co-elute within a single peak. Mass spectrometry is the usual way to access the molecular species identification and relative distribution.

In most studies, the chromatographic technique is developed to resolve the lipid classes present in a sample or a group of samples. For example some method are designed to address animal tissues (heart, liver, brain, kidney…) but only few studies are assessed with samples of various origin (such as animal and vegetal).

In chronological order, Graeve's method [11], initially devoted to zooplankton analysis was further adapted by Gerits [12] for wheat lipids analysis during bread making. Graeve's method [11] is particularly effective for the analysis of nonpolar lipids. At the opposite, Gerits' solvent conditions offer a better separation for lipids of intermediate polarity such as glycolipids. Both these methods where derived from the work of Homan and Anderson [13] which studied lipids from animal tissues. Homan and Anderson, themselves, adapted the pioneering work of Christie issued in 1985 [10]. By comparing all these publications, one can easily notice the changes operated by theses authors and the subsequent tailoring of the separation to assess the complexity of specific samples. However, solvent programs are complex and it is difficult and almost impossible to synthetize all these experimental conditions to arrive at a compromise gathering the strength of both methods.

In this publication, our objective was to develop an almost universal method for the overall evaluation of the lipid classes present in natural samples regardless of their origin. Further, as NPLC is rather complex to develop due to subtle interactions between analytes and mobile and stationary phases, we tried to exemplify the effect of changes in the solvent program on the lipid class separation. Ref [9] shows that even in NPLC, the solvent program can be adapted from conventional LC to UHPLC and, we can expect the solvent conditions we propose should be transposable as well.

As already pointed out, ESI is the most represented ionization interface in lipidomic studies, presumably because RPLC and HILIC represent nearly 80% of the chromatographic separations and are known to be compatible with this interface. Mobile phase compatibility with atmospheric pressure ionization (API) sources depends on the API source and the solvent [14].We investigated coupling our separation with ESI and APCI but also atmospheric pressure photoionization (APPI) in order to select the most appropriate interface. Finally, and because ELSD and corona charged aerosol detection (Corona-CAD®) are useful to monitor the separation in parallel with MS, a short comparison between those two detectors is provided.

2. Experimental

2.1. Chemicals

Isooctane, ethyl acetate, acetone (all HPLC grade), acetic acid (AA) and trimethylamine (TEA) were all purchased from Sigma-Aldrich. Chloroform and water (all HPLC grade) were obtained from VWR (Fontenay-sous-Bois, France). Isopropanol (IPA) (ULC/MS grade) was from Biosolve (Dieuze, France).

Isooctane was purified prior analysis by pumping the solvent through a semi preparative column packed with Lichroprep Si 60 5-20µm silica (Merck KGaA, Darmstadt, Germany).

2.2. Standards

Phosphatidylglycerols (PG), phosphatidylethanolamines (PE), phosphatidic acids (PA), phosphatidylcholines (PC), sphingomyelins (SM), lysophosphatidylcholines (LPC) from egg yolk, phosphatidylinositols (PI) from bovine liver, phosphatidylserines (PS) from bovine brain, Cardiolipins (CL) from bovine heart, squalene (SQ), cholesteryl palmitic acid (CE(16:0)), methyl-nonadecanoic acid (FAME), tristearic acid triglyceride (TG(18:0/18:0/18:0)), cholesterol (Chol), diacylglycerols (DG(18:2/0:0/18:2) and DG(16:0/16:0/0:0)), stearic acid (FA(18:0)), monoacylglycerol (MG(18:0/0:0/0:0)) were purchased from Sigma-Aldrich (St. Quentin Fallavier, France). Monogalactosyldiglycerols (MGDG) and digalactosyldiglycerols (DGDG) (vegetable origin) was from Avanti Polar (Coger, Paris, France). Wheat Glucosylceramides (GlcCer) were purchased from Extrasynthese (Genay, France). Acylated steryl glycosides (ASG (18:2-Glc-Sitosterol)) came from Larodan (Limhamn,Sweden) Ceramides: CerII (Cer(d18:1/18:0)), CerIIIb (Cer(t18:0/18:1)), CerVI (Cer(t18:0/18:0(2OH))), were purchased from Degussa (Hanau, Germany) and CerV (Cer(d18:1/18:0(2OH))) from Matreya (State College, PA USA). Stock solutions (5 g/L) of each standard compound were prepared in chloroform.

Table 1 presents detailed information about the lipid species composition of standards.

The lipid nomenclature follows the LIPID MAPS system and the shorthand notation for lipid structures [15]. When no abbreviation can be found for a specific lipid class or subclass in the LIPID MAPS nomenclature, commonly used abbreviation was employed (squalene (SQ), cholesterol (Chol), fatty acids methyl esters (FAME)). A list of abbreviations is proposed in table S-1.

2.3. Samples

Total lipid extracts from heart, brain and liver (all from bovine origin), *Escherichia coli*, yeast (*Saccharomyces cerevisiae*) and soybean were purchased from Avanti Polar (Coger, Paris, France). Lipowheat® oil is the food grade ingredient from ROBERTET Health & Beauty (Formerly HITEX, Vannes, France). This sample comes from the ethanolic extraction of bakery wheat gluten.
Each sample is prepared in chloroform at the concentration of 5 g/L for analysis and storage.

2.3.1. Lipid test mixtures

Test mixture 1 is composed by 22 lipid standards: SQ, CE, FAME, TG, Chol, DG 1-3, DG 1-2, FA, MG, ASG, MGDG, GlcCer, DGDG, PG, PE, PA, PI, CL, PS, PC, SM and LPC at an individual concentration of 0.5 g/L.

Test mixture 2 is a mixture of wheat oil (Lipowheat® oil) and soya lecithin supplemented with Chol in (9:9:0.6, v/v) proportion with a total lipid concentration of 10 g/L.

Ceramides test mixture 3 is made of CerII, CerIIIb, CerV and CerVI sub-classes at an individual concentration of 0.5 g/L.

Test mixture 1, 2 and 3 were prepared by mixing the appropriate stock solutions. After mixing all standards, the solution is evaporated under a stream of nitrogen and dissolved in mobile phase A: chloroform (4:1 v/v)

2.4. Apparatus

Separation of lipids was performed with an Inertsil Si 5µm (150 mm ×2.1 mm I.D.) column (GL Sciences Inc., Tokyo, Japan) thermostated at 40°C. The HPLC instrumentation consisted of an Agilent system, 1050 injector and a 1260 pump (Agilent Technologies, Santa Clara, CA, USA). An overpressure of 0.2 bar was applied to the mobile phase A reservoir. The 0.2 bar overpressure is set by a pressure regulator and the nitrogen line connected to the solvent bottle via a solvent pressurization kit obtained from Thermo Fischer Scientific. This kit consists in an adapted bottle cap and all necessary connections.

Two universal detectors, ELSD (Eurosep, Cergy, France) and Corona CAD® systems (both from ESA, Chelmsford, MA, USA) are compared; the signal was acquired with a Chromeleon data station (Thermo Fisher Scientific, Villebon-sur-Yvette, France). ELSD settings: nebulizer temperature 35°C, drift tube 45°C, photomultiplier 600 and air pressure 1.5 bars. Corona-CAD® settings: range 500pA, filter none and air pressure 35 psi.

MS analyses were performed with a LTQ-Orbitrap Velos Pro (Thermo Fisher Scientific). The MS^2 and MS^3 spectra were obtained in data dependent acquisition (DDA) mode. The LTQ-Orbitrap Velos Pro mass spectrometer was equipped with an H-ESI II probe / and a combined APCI/APPI ion source.

2.5. Chromatographic method

The mobile phases and the solvent program are presented in table 2. The flow rate was set at 0.8 $mL.min^{-1}$. The injected volume was 2 µL.

2.6. MS method

H-ESI II probe: Spray voltage was set at 3.3 kV. Heater temperature of the probe was set at 300°C. Sheath gas, auxiliary gas, and sweep gas flow rates were set at 40, 20, and 0 (arbitrary unit) respectively. Capillary temperature was set at 350°C and S-lens RF level at 60%. Analysis was performed in negative and positive ion mode.

APCI/APPI ion source: Corona needle voltage in APCI mode was set at 6 kV. Vaporizer temperature of the probe was set at 400°C. Sheath gas, auxiliary gas, and sweep gas flow rates were set at 40, 10, and 0 (arbitrary unit) respectively. Capillary temperature was set at 325°C and S-lens RF level at 60%. Analyses were performed in negative and positive ion mode.

3. Results and Discussion

There are two ways to understand the different NPLC methods developed for lipid class analysis and their progress over time: either by the sample origin or by the stationary phase and solvent program.
Table 3, summarize the successive evolutions of Christie's method by the authors quoted in the introductive part of the manuscript. Chloroform, a CMR (carcinogenic, mutagenic, or toxic for reproduction) solvent was replaced by dichloromethane, itself substituted by the less toxic and peek-tubing compatible ethyl acetate. IPA was replaced by acetone to improve the sterols (ST)/DG chromatographic selectivity. AA and TEA were added at the end of the gradient program to enhance phospholipids (PL) analysis. In the same way, the addition of 0.2% (v/v) of ethyl acetate in isooctane appeared to improve the separation of early eluting lipids. Other modifications/improvements were made to help instrument performances. IPA was used as a rinsing solvent, prior the equilibration with isooctane and to avoid pumping failure with this low viscosity solvent that can be encountered with some pumping devices.

The mobile phases used in Graeve's [11] and Gerits' [12] methods differ by the presence of 0.2% (v/v) of ethyl acetate in isooctane, the ionic modifiers concentration and the addition of IPA as rinsing solvent (table 3). In the present study, we intended to appreciate and exemplify the impact of these differences on the chromatographic separation of lipid classes. The main goal being to achieve the highest degree of separation allowing the characterization of biological lipid extracts from various origins (animal, vegetal, yeast, bacteria). For this purpose, test mixture 1 composed of 22 lipid standards and test mixture 2 were systematically chromatographed. Ceramides are biologically relevant lipids which have not been considered in refs [11,12]. We used test mixture 3, to appreciate the impact of the changes in chromatographic conditions on the retention of several compounds of this class.

The different methods listed in table 3 use ELSD as detection principle. In this study, we compared the chromatographic profiles achieved by both ELSD and Corona-CAD®. Those two quasi-universal detectors allow quantitation but are unable to provide any structural information. As this later aspect is mandatory in lipidomic profiling of biological extracts, we assessed the MS response when coupling our separation through three ionization sources, namely ESI, APCI and APPI.

Finally, 7 total lipid extracts from different origins (3 animal, 2 vegetal, 1 from yeast and 1 from bacteria) were analyzed with the method presenting the best resolution between the lipid classes. In order to appreciate the versatility of the method we briefly compared the results obtained with each extract to information from the literature.

3.1. Mobile phase composition

3.1.1. Mobile phase A

Isooctane purification

In an attempt to reduce the impurity level, isooctane was flowed through a semi-preparative column packed with Lichrospher Si-60, 5-20 µm bare silica prior its use in mobile phase [16–18].

Eluent pressurization

Gerits introduced the IPA rinsing to prevent pressure fluctuation encountered at the beginning and at the end of the solvent program. From our experience, such phenomenon is more or less pronounced depending on the equipment used and is encountered with highly compressible and low viscosity solvents such as alkanes. A slight pressurization (0.2 bar) of the solvent reservoir minimize the pumping difficulties encountered with alcanes.

Ethyl acetate

Graeve's method [11] allows the best separation of the most nonpolar lipids (SQ, SE (sterol ester), WE (wax ester), FAME, DAGE (diacylglycerol ethers) and TG). Mobile phase A composition is isooctane:ethyl acetate (99.8:0.2, v/v). Ethyl acetate was preferred to tetrahydrofuran (THF) initially proposed by Christie or Homan since it is compatible with peek tubing [19]. The lower polarity and the selectivity change induced by this solvent allow an improved separation of SQ, SE and WE.

Gerits [12] uses pure isooctane. Unfortunately, the most nonpolar lipids cannot be seen on its chromatograms that start at 5 min after the injection. In order to appreciate the exact role of the 0.2% (v/v) ethyl acetate addition in mobile phase A, test mixtures 1 and 2 were analyzed with a pure or modified phase A (figure 1). Adding 0.2% (v/v) ethyl acetate only influences the selectivity between lipid classes eluted during the first 5 minutes of the chromatogram. Both SE and FAME are less retained and show a broader peak. Additionally, the resolution between the dead volume and SQ decreases. The chromatograms from natural samples mixture show an improved separation of nonpolar compounds eluted during the 5 first minutes. Co-elutions with solvent impurities are also limited.

To summarize, the addition of 0.2% (v/v) ethyl acetate enhances the discrimination of nonpolar lipids. Alternatively, when SQ is a compound of interest, only pure isooctane used as initial mobile phase allows its retention.

3.1.2. Mobile phase B

The mobile phase B, as optimized by Gerits for the analysis of medium polarity lipids (MG, MGDG and DGDG), contains 20 fold more AA than the mobile phase proposed by Graeve [11]. In order to highlight the effect of AA on lipid classes retention, three levels were compared and presented in figure 2: 0.02% (Graeve), 0.15 % (v/v) (this work) and 0.4% (Gerits).

The retention of FA decreases with increasing concentration in AA in the mobile phase. This is probably due to the competition between AA and FA for the adsorption onto the stationary phase. With 0.02% AA (v/v), the FA peak co-elutes with a system peak and at 0.4% (v/v) FA and DG 1,3 co-elute. Among the tested concentrations, 0.15% AA (v/v) offers the best compromise for the elution of FA and their resolution with adjacent peaks.

In addition, AA concentration in mobile phase B has a noticeable impact on the second part of the chromatogram. 0.15% AA (v/v) is also an optimum concentration for the elution of PL at the end of the chromatogram as advisable from chromatographic profile of test mixture 1 in figure 2. Alternatively, using 0.4% AA (v/v) is interesting to improve the chromatographic profile of lipids eluting between DGDG and PL.

We decided to favor FA retention and PL separation and thus, to use the intermediate 0.15% AA (v/v) concentration in the solvent program.

3.1.3. Mobile phase C

Homan [13] first introduced a mobile phase C composed by IPA and water (85:15, v/v) with an equimolar amount of AA and ethanolamine (EA) at 7.5 mM. The same C mobile phase is used by Graeve [11] . The experimental conditions of Gerits [12] are close to those of Homan, except EA is replaced by TEA. The mobile phases proposed by Homan [6] don’t incorporate any ionic modifier. In order to understand the influence of the ion pair concentration and volume ratio in mobile phase C, a separation of test mixtures 1 and 2 with A: 0.05% (v/v) AA and TEA, B: 7.5 mM AA and TEA (0.043% (v/v) AA and 0.104% (v/v) TEA) C: neither AA nor TEA is presented in figure 3.

The AA/TEA relative amounts do not affect the lipids eluted at the beginning of the chromatogram with the notable exception of FA. When absent or in equimolar ratio, FA retention is unaffected.
When the same volume of AA and TEA e.g. 0.05% (v/v) is added, the molar excess of AA represents the

addition of 0.025% (v/v) AA in the mobile phase. Although being present in the C mobile phase and despite of the rinsing phase D, the AA amount influences the FA retention at the beginning of the chromatogram. In these conditions, the AA amount in phase C is responsible for the co-elution of FA and Chol.
The relative amounts of AA and TEA influence polar lipid (PL) retention and selectivity. The best separation is obtained with an equimolar amount of AA/TEA in phase C.

3.1.4. Mobile phase D

Graeve's method [11] doesn't make use of a particular rinsing solvent at the end of the solvent program. After the phase C step, the solvent program goes back to the B phase and then re-equilibration is performed using the A phase. The low viscosity of isooctane together with the high permeability of monolithic silica, allow doubling the flow rate during the equilibration step. Gerits [12] introduced IPA as rinsing solvent and indicated that this rinsing step improves the subsequent pumping of isooctane. As already underlined, this step influences the first part of the chromatogram.

In this study, a rinsing step was introduced with ethyl acetate, an intermediate polarity solvent, in order to facilitate equilibration while favoring the retention of nonpolar lipids at the beginning of the chromatogram. As indicated in table 2, the rinsing step consists in a 50:50 mixture between mobile phase A and D. The chromatograms of test mixtures 1 and 2 obtained with 3 rinsing conditions are presented in figure 4. When no rinsing is performed (Fig 4.B), mobile phase D composition is identical to mobile phase A. In figure 4.A and 4.C, IPA and ethyl acetate are respectively used.

As seen in Figure 4.A the use of IPA as rinsing solvent is not compatible with a proper retention of neutral lipids at the beginning of the chromatogram. Indeed, we can hypothesize that the IPA adsorption energy is so high that this solvent cannot be readily driven out the silanols of the silica by isooctane.

Repeated experiments have shown that the ethyl acetate rinsing step (Fig 4.C) gives a superior result compared to an increase in equilibration time performed with mobile phase A (Fig 4 A). In the first part of the chromatogram, SQ, CE, FAME and TG are more retained. The retention time of FA is slightly increased but the influence of the ethyl acetate rinsing step is especially noticeable on peak geometry with FA eluting as a sharp and intense peak.

It is also important to note that the rinsing step can have an influence on the most polar lipids of the chromatogram. The PL profile in figure 4.A using IPA is noticeably different than the profiles obtained with mobile phase A (Fig 4.B) and ethyl acetate (Fig 4.C).

Solvent consumption is directly impacting analysis cost and solvent rejection being an environmental and safety issue, it is worthy to note that the method we propose use about 40% less solvent than refs [10-11].

The total solvent volume of our method is 42 mL, 32 mL for the solvent program plus 10 mL for rinsing and equilibration whereas it is 68 mL when using the methods described in refs [10-11].

Medium polarity lipids (Ceramides) The aforementioned publications do not relate to ceramides.This lipid class is frequently investigated in lipidomic studies, especially in skin research where a vast diversity is encountered [23–26]. We considered important to evaluate the elution window of the ceramide subclasses and to assess the possible co-elution with other lipid classes. Cer elute in the area of medium polarity lipids with retention times intermediate between MG and MGDG (figure 6). ASG co-elutes with the first peak of CerVI. CerV elutes as a double peak. CerV, a synthetic ceramide, is a racemic mixture of two epimers N-(R,S)-alpha-Hydroxyoctadecanoyl-D-erythro-sphingosine. These two peaks presumably correspond to the epimers. Bare silica had already proven to separate epimers, as for example sterols [27]. No information is available about the stereochemistry of CerVI, but, as for CerV, its elution as two distinct peaks may be due to the occurrence of two epimeric forms. Unlike in CerV and CerVI, carbon at position 2 of the fatty acyl chain of CerII is not a chiral center. The double peak encountered with this compound is presumably due to the Z and E configuration of the double bound of the fatty base moiety. To facilitate understanding, drawings of the chemical structures are presented in figure S-1. The MS spectra of the 3 couples of peaks are commented further in the document (ESI, APCI and APPI comparison).

3.2. ELSD / Corona-CAD® comparison

ELSD has gained a wide acceptance in lipid class analysis since the pioneering work of Robinson and Macrae [20] at the beginning of the ‘80s. Indeed, ELSD is a nebulization-based detector that is compatible with gradient elution and allows detecting any solute less volatile than the mobile phase. The Corona-CAD®, introduced in 2004 [21], shares the same operating principle except aerosol charging is used instead of the light diffusion exploited in the ELSD.

Figure 5 presents the chromatograms of test mixtures 1 & 2 at 0.5 g/L (2µL injected) using both detectors. Corona-CAD® appears to be more sensitive to the baseline drift phenomenon occurring from the gradient program. The chromatogram of lipid standard at equal concentration (test mixture 1) shows more consistent peak heights with Corona-CAD® than with ELSD. This can be explained by the typical response functions of both detectors [22]. With ELSD, when Rayleigh scattering is the dominant phenomenon, the sensitivity increases with increasing amount of solutes. From our experience, this is the case when narrow bore column and reduced flow rates are used. Consequently, the peak intensities of minor compounds appear to be less than their actual quantity. At the opposite, major compounds benefit from the increased sensitivity and their peak intensities dominate the chromatogram. The response function of the Corona-CAD® is more consistent among injected quantities and, at least, the sensitivity decreases for high solute amounts. Therefore, with the

Corona-CAD®, the chromatographic profile is more likely to reflect the relative amounts of solutes involved in complex samples such as mixture 2.

3.3. ESI, APCI and APPI comparison

Although combined positive-negative ionization mode could be achieved by the mass spectrometer, distinct positive and negative profiles where recorded with the three ion sources to highlight the different behavior of some lipid classes (figure 7).

ESI does not give any signal at the beginning of the chromatogram in either positive or negative ionization mode. Only polar lipids are detected but with an unfavorable background noise. Coupling the present NPLC method with ESI cannot be recommended.

The chromatograms acquired with either APCI or APPI showed similar profiles. In positive ion mode, peak intensities of ionized lipid classes appeared to be similar. On the contrary, APPI delivered a 4 fold more important signal than APCI in negative mode. APCI is much more readily available in mass spectrometry platforms than APPI and can conveniently be used with this method. However, APPI will be preferred if available. For example, the Cer class is detected with a ≈20 fold more intense response in negative APPI detection compared to positive APPI (figure 8). This finding corroborates the fact that APPI appears to be particularly interesting for lipid analysis [29], well suited to NPLC solvent conditions [30] and offering a high sensitivity for lipid analysis [31].

The three API sources were compared by Imbert et al. [14] by coupling the Graeve's method [11] to mass spectrometry for the analysis of *Leishmania donovani* lipids. In this previous study from our group, the number of lipids classes was twice as less. In addition, when comparing chromatographic profiles, the separation appears to be poorer than in the present study. It is worthy to note that mobile phases contain AA and TEA in proportions that are different from the present study and this presumably influence ionization. In addition, Imbert and al. employed an acetone post-column addition as dopant for APPI ionization. In the present study, such addition did not improve ionization. The presence of 0.2% (v/v) ethyl acetate in the initial mobile phase presumably plays this role. The effect of eluent composition on the ionization efficiency of ESI, APCI and APPI in LC–MS was studied in [32].

Figure 9 contains a selection of MS spectra obtained for 4 standards that illustrate characteristic ions obtained with the 3 API sources. Supplementary figure S-2 presents the LC/MS full scan spectra of all standards considered in this study in either positive or negative ionization mode with ESI, APCI and APPI interfaces.

3.3.1. CerIIIb : Cer(t18 :0/18 :1)

The three API sources produced similar ions for CerIIIb. The full scan spectra of other Cer standards presented similar ionization patterns.

In negative mode [33,34], the most abundant ion was $[M-H]^-$ whereas the AA adduct $[M-H+CH_3COOH]^-$ was also observed. With ESI, the AA adduct represented 80% relatively to the $[M-H]^-$ but only 20% when APCI and APPI were used. The total ion count (TIC) was low with ESI^- (2.6E4) whereas it was more important with APCI and APPI. APPI provided a 2 fold more intense signal than APCI.

In positive mode, the most abundant ion was $[M+H]^+$ and was accompanied by the $[M+H-H_2O]^+$ that correspond to the loss of a water molecule. This in source fragmentation was more pronounced with APPI and less important with ESI. The TIC remained low in ESI (6.3E4) and more important with APCI and APPI. At the opposite of the negative mode, the TIC was 2 fold more important with APCI than APPI.

The MS spectra obtained in full scan, MS^2 and MS^3 for each couple of peaks encountered with CerV and CerVI were identical (figure S-3). The MS spectra of the two peaks of CerII showed the same ions but with different relative intensities. This supposes quasi-identical structures and reinforces the hypothesis of the epimeric forms separation or CerV and CerVI and the stereoisomerism of CerII.

3.3.2. ASG(18:2-Glc-Sitosterol)

In negative mode, the base peak was $[M-H+CH_3COOH]^-$ with the 3 ionization sources. Here also, APPI provided a 3 fold more intense signal than APCI, whereas ESI exhibited a low TIC (1.2E4).

In positive mode [35], the ASG ions could not be retrieved from the ESI LC/MS profile. The most abundant ion corresponds to $[M-FA-sugar+H+H2O]^+$ and was 3 fold more intense with APPI compared to APCI.

3.3.3. PA from egg yolk, PA(16:0_18:1) as most abundant specie.

The adducts and fragmentation patterns observed with PA were also encountered with other PL (PG, PE, PI and PS) [36,37].

In negative mode, the base peak was $[M-H]^-$ with all API sources. The TIC was comparable between ESI and APCI (about 1E7) and 4 fold more abundant with APPI.

In positive mode, the observed ions with ESI were different from the two other sources. TEA adducts were observed with ESI as $[M+TEA+H]^+$ et $[M+2TEA+H]^+$. With both APCI and APPI, the major ion corresponded to the loss of the polar head of the PL $[M+H\text{-polar head}]^+$ and a $[M+Na]^+$ of lesser intensity was also observed.

3.3.4. PC from egg yolk, PC(16:0_18:1) as most abundant specie

The adducts and fragmentation patterns observed with PC were also encountered with other PL (SM and LPC) [36,37].

In negative mode, ESI spectra were different from the two others and exhibited a predominant AA adduct. With APCI and APPI, a radical ion $[M°]^-$ was observed together with a $[M-CH_3]^-$ that correspond to the loss of a methyl group. The signal intensity was comparable between ESI and APCI (about 3E6) and 5 fold more intense with APPI.

In positive mode, the major ion was [M+H]+ with ESI and no fragment ion was observable. With APCI and APPI, the major ion was a $[M+H\text{-polar Head}]^+$ and $[M+H]^+$ was also observed. The signal intensity was comparable between the 3 API sources.

It is important to note that, whereas APCI and APPI induce more fragments than ESI, the structural information is preserved by combining both positive and negative mode of ionization.

3.3.5. The particular case of TG

Tristearin or TG(18:0/18:0/18:0) was arbitrary chosen to represent the TG class. The LC/MS tristearin spectra obtained with APCI and APPI in positive mode showed an unique $[M+H\text{-FA}]^+$ ion whereas in TG spectra from lipid samples, the $[M+H\text{-FA}]^+$ coexisted with the $[M+H]^+$. TG from natural oils are often characterized using the $[M+H]^+$ ion [17,18]. In most publications, saturated TG are not reported. Saturated TG are indeed only present in very low amount in natural oils. A systematic study of TG fragmentation patterns using LC/APCI-MS shows that for saturated TG the $[M+H]^+$ ion is not observed [40]. For TG(18:1/18:1/18:1) or TG(16:1/16:1/16:1)) the $[M+H]^+$ is weak and accounts for only 7% of the base peak $[M+H\text{-FA}]^+$. The $[M+H]^+$ ion becomes the major ion of the spectrum when the degree of unsaturation increases.

To summarize, APPI appeared to be the best-suited interface for coupling the present NPLC lipid classes separation to mass spectrometry. A simplified list of ions encountered in positive and negative ion mode APPI is presented in table 4. This table was built to facilitate the identification of lipid classes in different sample types. In most cases, the lipid classes correspond to analytical standard. In some instances, when the standards are not readily available, the reported ions correspond to lipid structures identified in natural samples. For each lipid class or subclasses, the ions observed for a representative specie are reported together with its molecular mass, retention time and adduct(s) observed. By working with the two ionization modes, all the lipid classes studied herein could be detected. It is easily possible to trace back to the lipid specie parent structure despite of the in source fragmentation.

3.4. Chromatographic profiles of 7 total lipid extracts from differerent samples

All total lipid extracts available from Avanti Polar were studied: 3 from animal, 2 from plants and one from yeast and bacterium (figure 10).

3.4.1. Heart / Liver / Brain

Homan [13] studied the three animal tissues, Christie [10] and McLaren [9] studied the heart and liver, and Holčapek's group [6] the brain. The three animal samples exhibit similar lipid profiles. TG, Chol, FA are found in variable quantities according to the animal tissue considered. PE and PC are the major phospholipids. Heart shows a higher amount of CL whereas brain contains high quantities of cerebrosides (HexCer and HexCer(OH)) that are not present in other tissues. The lipid profiles obtained in the present study are similar to those shown by Christie [10] or Homan [13]. The method proposed in herein presents a better retention of CE and allows quantifying them if needed. In McLaren's study, the aim was to analyze the major lipids with the shortest possible analysis time. Consequently, the chromatogram duration is only 10 minutes but low concentration lipids are not observable in the chromatograms of real samples. This is possibly a consequence of the reduced amount of sample injected. As the method was developed with only 7 different lipid standards, it is difficult to appreciate the real ability of this method to separate a complex total lipid extract. In contrast, the UHPSFC-MS profile of pork brain presented by [6], shows a very detailed separation. All the lipids we evidenced in our profiles (except SQ) were found and additional lipids in low amount were identified.

UHPSFC-MS appears to be a very promising technique for total lipid extract analysis together by its high efficiency and high throughput. It is also worthy to note that this technique only uses supercritical CO2 with methanol and water as co-solvent or make-up fluid and is much more environment friendly than usual NP-HPLC methods. At the present time, this equipment is scarcely present in the laboratories but these uses should grow for both high throughput and extensive analysis.

3.4.2. Soybean / Wheat

The two vegetal samples soya and wheat are also the most complex samples involved in this study in term of lipid composition. They are particularly rich in lipid of intermediate polarity typical from vegetal such as ASG, SG, GlcCer and DGDG. Soya lecithin and wheat were already extensively studied in our laboratory while developing separations with the poly(vinyl)alcool stationary phase [41] and ASG, SG, GlcCER, DGDG, PI, PE and PC were identified.

Soya lecithin is particularly rich in PL and most studies focus on these classes. An example of extensive characterization using phosphorus 31 nuclear magnetic resonance can be found in [42] and the lipid classes reported are PC, PE, PI, PA, PG, N-acylphosphatidylethanolamines (NAPE), LPC, diphosphatidylglycerol (DPG), PS and lysophosphatidic acids (LPA) (by increasing order of magnitude in the sample). The

chromatographic profiles in figure 10 show that, whereas the main classes are identified, our method only fails at detecting the quantitatively minor lipid classes. Those minor classes (LPC, DPG, PS and LPA) are less than 0.8% mol/100 mol of phosphorylated lipids.

Concerning wheat lipids, the entirety of the lipid classes involved in Gerits' publication [12] are resolved in our conditions. In addition, 6 extra lipids are identified (SQ, SE, ST, ASG, SG and GlcCer) and 4 unknown peaks are resolved from the lipid classes. Compared to previously published solvent programs, the present chromatographic conditions allow an appropriate retention of the nonpolar lipid classes (SQ and SE) together with an improved separation in the intermediate polarity lipids area which allows to detect ST, ASG, SG and GlcCer while preserving the resolution of PL classes.

3.4.3. Yeast (Saccharomyces cerevisiae)

Saccharomyces cerevisiae is often used as a model organism and there is abundant information concerning its metabolism. The lipid profile of yeast (*Saccharomyces cerevisiae*) was not studied by the authors we comparedwith and we referred to other bibliographical sources to ascertain the level of information provided by our method. The yeast lipidome was investigated by shotgun mass spectrometry in ref [43] with a special attention paid to lyso forms of the PL classes. Ref [44] also examines yeast lipidome and presents consistent results (only Cer are found in addition to the lipids of Ref [43]). The main lipid classes highlighted in these articles were TG, DG, Cer and ST and the phospholipids PA, PS, PE, PC, PI, PG, CL together with their lyso forms. Inositol phosphoceramide (IPC) derivatives (IPC, Mannosylated-IPC and $Man(IP)_2C$) were found in notable but also variable amount in *S. cerevisiae* wildtype stains.

Our method allowed identifying the main lipid classes (except PS and the lyso-forms, which was not in noticeable quantity in our sample) but not the IPC derivatives. This result compared favorably with the NPLC/Corona-CAD® of ref [45]. SQ, coenzyme Q6 and PG are detected in our chromatographic profile and are not reported in [45].

Neither our method nor [45] allow to detect IPC derivatives. Except in the 12-14 min range no unidentified peak could be detected and this elution window does not correspond to the IPC derivatives that, from our experience [46], should elute near the PL elution windows. We unsuccessfully performed an in depth examination of the APPI profiles searching for the quasi-molecular and possible adduct ions of the main species of IPC and its derivatives. IPC derivatives are cell messengers and appear to increase dramatically as a response to a stress or a change in the culture media (temperature for [44], AA for [47]). Their levels are possibly too low to be detected in our sample. These compounds are also ionized very differently according to the ionic modifiers added to the mobile phase both with respect to the adducts observed and their intensities [36,41]. A detailed investigation of IPC derivatives detection under our mobile phase composition conditions would be necessary but is out of the scope of this work.

3.4.4. Bacteria (Escherichia coli)

As for yeast, no NPLC of the *E. coli* lipids was found and the characteristic composition of these bacteria had to be retrieved from the literature. The typical composition as mentioned by the lipid standard supplier Avanti Polar is rather simple and *E.coli* extract contains 57.5% PE, 15.1% PG, 9.8 CL and 17.6% of non-identified lipids. Coenzyme Q8 [49] is not listed but is also present and signaled as being obtained from *E. coli* extract by the same supplier. Lipid A which is involved in the toxicity of Gram negative bacteria is also present in *E. coli* but wasn't detected in our experimental conditions as the *m/z* of its molecular ion is beyond the mass range of the full scan detection (*m/z* 1700). This lipid composition was confirmed by different publications using mass spectrometry [50–52] and our separation appeared to highlight the main component of the *E. coli* extract.

4. Conclusions

Most of NPLC methods for lipid classes analysis where developed to separate lipids issued from animal samples. Fewer methods were developed to assess the higher complexity of vegetal samples. Some plant lipids such as ASG, MGDG, SG and DGDG present an intermediate polarity and increase the sample complexity in this region of the chromatogram.

The method we propose compares favorably with those developed for animal tissues [9–11,13] and presents an improved separation for vegetal samples [12]. This method, developed using lipid classes of intermediate polarity is also interesting to separate ceramides.

NPLC method development is generally considered as difficult and requiring a specific skill. We decided to add information about the different issues solved during this development. Particularly the use of nonpolar, low viscosity solvent such as isooctane and the use of a pressurized solvent tank to circumvent the pumping difficulties encountered. In addition, the presence of impurities in isooctane led us to re-purify this solvent using a semi-preparative silica column. We also focused on the rinsing step and the importance of using ethyl acetate to both eliminate the C mobile phase from the stationary phase and favor the re-equilibration.

NPLC solvent programs frequently incorporate complex mobile phases. In this study, we documented the importance of adding 0.2% (v/v) ethyl acetate in the initial mobile phase. Also, the importance of the relative amounts of AA and TEA in the mobile phase on the retention of some specific lipid classes such as FA in the first part of the chromatogram but also the PL classes at the end and the compromise to be found to ensure a correct selectivity.

The comparison of the detection systems that are both heavily solvent dependent reinforce the interest of the Corona-CAD® thanks to its increased sensitivity at low concentration compared to the commonly used ELSD. When comparing the API interfaces under NPLC conditions, ESI did not succeed at detecting the whole lipids in the chromatogram as signal extinction occurs at the beginning of the chromatogram. We have shown that for lipids such as PL, in positive mode APCI and APPI present more in source fragmentation compared with ESI. In negative mode, the in source fragmentation is comparable with the three API sources. By using both positive and negative mode, structural information is visible in full scan spectra. Coupling with APCI provided satisfactory results but APPI is generally more sensitive and does not require any dopant make-up in our chromatographic conditions.

References

[1] S. Subramaniam, E. Fahy, S. Gupta, M. Sud, R.W. Byrnes, D. Cotter, A.R. Dinasarapu, M.R. Maurya, Bioinformatics and Systems Biology of the Lipidome, Chem. Rev. 111 (2011) 6452–6490.

[2] E. Fahy, S. Subramaniam, R.C. Murphy, M. Nishijima, C.R.H. Raetz, T. Shimizu, F. Spener, G. van Meer, M.J.O. Wakelam, E.A. Dennis, Update of the LIPID MAPS comprehensive classification system for lipids, J. Lipid Res. 50 (2008) S9–S14.

[3] T. Cajka, O. Fiehn, Comprehensive analysis of lipids in biological systems by liquid chromatography-mass spectrometry, TrAC Trends Anal. Chem. 61 (2014) 192–206.

[4] E. Cífková, R. Hájek, M. Lísa, M. Holčapek, Hydrophilic interaction liquid chromatography–mass spectrometry of (lyso)phosphatidic acids, (lyso)phosphatidylserines and other lipid classes, J. Chromatogr. A. 1439 (2016) 65–73.

[5] M. Holčapek, E. Cífková, B. Červená, M. Lísa, J. Vostálová, J. Galuszka, Determination of nonpolar and polar lipid classes in human plasma, erythrocytes and plasma lipoprotein fractions using ultrahigh-performance liquid chromatography-mass spectrometry, J. Chromatogr. A. 1377 (2015) 85–91.

[6] M. Lísa, M. Holčapek, High-Throughput and Comprehensive Lipidomic Analysis Using Ultrahigh-Performance Supercritical Fluid Chromatography–Mass Spectrometry, Anal. Chem. 87 (2015) 7187–7195.

[7] M. Holčapek, M. Ovčačíková, M. Lísa, E. Cífková, T. Hájek, Continuous comprehensive two-dimensional liquid chromatography-electrospray ionization mass spectrometry of complex lipidomic samples, Anal. Bioanal. Chem. 407 (2015) 5033–5043.

[8] M. Šala, M. Lísa, J.L. Campbell, M. Holčapek, Determination of triacylglycerol regioisomers using differential mobility spectrometry, Rapid Commun. Mass Spectrom. RCM. 30 (2016) 256–264.

[9] D.G. McLaren, P.L. Miller, M.E. Lassman, J.M. Castro-Perez, B.K. Hubbard, T.P. Roddy, An ultraperformance liquid chromatography method for the normal-phase separation of lipids, Anal. Biochem. 414 (2011) 266–272.

[10] W.W. Christie, Rapid separation and quantification of lipid classes by high performance liquid chromatography and mass (light-scattering) detection., J. Lipid Res. 26 (1985) 507–512.

[11] M. Graeve, D. Janssen, Improved separation and quantification of neutral and polar lipid classes by HPLC–ELSD using a monolithic silica phase: Application to exceptional marine lipids, J. Chromatogr. B. 877 (2009) 1815–1819.

[12] L.R. Gerits, B. Pareyt, J.A. Delcour, Single run HPLC separation coupled to evaporative light scattering detection unravels wheat flour endogenous lipid redistribution during bread dough making, LWT - Food Sci. Technol. 53 (2013) 426–433.

[13] R. Homan, M.K. Anderson, Rapid separation and quantitation of combined neutral and polar lipid classes by high-performance liquid chromatography and evaporative light-scattering mass detection, J. Chromatogr. B. Biomed. Sci. App. 708 (1998) 21–26.

[14] L. Imbert, M. Gaudin, D. Libong, D. Touboul, S. Abreu, P.M. Loiseau, O. Laprévote, P. Chaminade, Comparison of electrospray ionization, atmospheric pressure chemical ionization and atmospheric pressure photoionization for a lipidomic analysis of Leishmania donovani, J. Chromatogr. A. 1242 (2012) 75–83.

[15] G. Liebisch, J.A. Vizcaino, H. Kofeler, M. Trotzmuller, W.J. Griffiths, G. Schmitz, F. Spener, M.J.O. Wakelam, Shorthand notation for lipid structures derived from mass spectrometry, J. Lipid Res. 54 (2013) 1523–1530.

[16] S. Williams, Ghost peaks in reversed-phase gradient HPLC: a review and update, J. Chromatogr. A. 1052 (2004) 1–11.

[17] T.J. Leiker, R.M. Barkley, R.C. Murphy, Analysis of diacylglycerol molecular species in cellular lipid extracts by normal-phase LC-electrospray mass spectrometry, Int. J. Mass Spectrom. 305 (2011) 103–108.

[18] X. Guo, A.P. Bruins, T.R. Covey, Characterization of typical chemical background interferences in atmospheric pressure ionization liquid chromatography-mass spectrometry, Rapid Commun. Mass Spectrom. 20 (2006) 3145–3150.

[19] S. Altmaier, K. Cabrera, Structure and performance of silica-based monolithic HPLC columns, J. Sep. Sci. 31 (2008) 2551–2559.
[20] J.L. Robinson, R. Macrae, Comparison of detection systems for the high-performance liquid chromatographic analysis of complex triglyceride mixtures, J. Chromatogr. 303 (1984) 386–390.
[21] R.W. Dixon, D.S. Peterson, Development and testing of a detection method for liquid chromatography based on aerosol charging, Anal. Chem. 74 (2002) 2930–2937.
[22] R.G. Ramos, D. Libong, M. Rakotomanga, K. Gaudin, P.M. Loiseau, P. Chaminade, Comparison between charged aerosol detection and light scattering detection for the analysis of Leishmania membrane phospholipids, J. Chromatogr. A. 1209 (2008) 88–94.
[23] D. Kauhanen, M. Sysi-Aho, K.M. Koistinen, R. Laaksonen, J. Sinisalo, K. Ekroos, Development and validation of a high-throughput LC–MS/MS assay for routine measurement of molecular ceramides, Anal. Bioanal. Chem. 408 (2016) 3475–3483.
[24] J. van Smeden, W.A. Boiten, T. Hankemeier, R. Rissmann, J.A. Bouwstra, R.J. Vreeken, Combined LC/MS-platform for analysis of all major stratum corneum lipids, and the profiling of skin substitutes, Biochim. Biophys. Acta BBA - Mol. Cell Biol. Lipids. 1841 (2014) 70–79.
[25] A. Tfayli, F. Bonnier, Z. Farhane, D. Libong, H.J. Byrne, A. Baillet-Guffroy, Comparison of structure and organization of cutaneous lipids in a reconstructed skin model and human skin: spectroscopic imaging and chromatographic profiling, Exp. Dermatol. 23 (2014) 441–443.
[26] L. Quinton, K. Gaudin, A. Baillet, P. Chaminade, Microanalytical systems for separations of stratum corneum ceramides, J. Sep. Sci. 29 (2006) 390–398.
[27] A. Sunde, P. Stenstad, K.B. Eik-Nes, Separation of epimeric 3-hydroxyandrostanes and 3-hydroxyandrostenes by thin-layer chromatography on silica gel, J. Chromatogr. A. 175 (1979) 219–221.
[28] S. Khoury, Theoretical and practical aspects of the quantification of lipid classes by use of universal detectors and mass spectrometry, PhD Thesis, Paris Saclay, 2015. http://www.theses.fr/2015SACLS191 (accessed February 13, 2017).
[29] I. Marchi, S. Rudaz, J.-L. Veuthey, Atmospheric pressure photoionization for coupling liquid-chromatography to mass spectrometry: A review, Talanta. 78 (2009) 1–18.
[30] S.-S. Cai, J.A. Syage, Comparison of Atmospheric Pressure Photoionization, Atmospheric Pressure Chemical Ionization, and Electrospray Ionization Mass Spectrometry for Analysis of Lipids, Anal. Chem. 78 (2006) 1191–1199.
[31] S.-S. Cai, J.A. Syage, Atmospheric pressure photoionization mass spectrometry for analysis of fatty acid and acylglycerol lipids, J. Chromatogr. A. 1110 (2006) 15–26.
[32] R. Kostiainen, T.J. Kauppila, Effect of eluent on the ionization process in liquid chromatography–mass spectrometry, J. Chromatogr. A. 1216 (2009) 685–699.
[33] M.H. Lee, G.H. Lee, J.S. Yoo, Analysis of ceramides in cosmetics by reversed-phase liquid chromatography/electrospray ionization mass spectrometry with collision-induced dissociation, Rapid Commun. Mass Spectrom. RCM. 17 (2003) 64–75.
[34] F.-F. Hsu, J. Turk, Characterization of ceramides by low energy collisional-activated dissociation tandem mass spectrometry with negative-ion electrospray ionization, J. Am. Soc. Mass Spectrom. 13 (2002) 558–570.
[35] R. Rozenberg, N.L. Ruibal-Mendieta, G. Petitjean, P. Cani, D.L. Delacroix, N.M. Delzenne, M. Meurens, J. Quetin-Leclercq, J.-L. Habib-Jiwan, Phytosterol analysis and characterization in spelt (Triticum aestivum ssp. spelta L.) and wheat (T. aestivum L.) lipids by LC/APCI-MS, J. Cereal Sci. 38 (2003) 189–197.
[36] M. Pulfer, R.C. Murphy, Electrospray mass spectrometry of phospholipids, Mass Spectrom. Rev. 22 (2003) 332–364.
[37] R.C. Murphy, Tandem Mass Spectrometry of Lipids, 2014. http://pubs.rsc.org/en/content/ebook/978-1-84973-827-9#!divbookcontent (accessed February 22, 2017).
[38] E. Kofroňová, J. Cvačka, P. Jiroš, D. Sỳkora, I. Valterová, Analysis of insect triacylglycerols using liquid chromatography-atmospheric pressure chemical ionization-mass spectrometry, Eur. J. Lipid Sci. Technol. 111 (2009) 519–525.

[39] M. Fasciotti, A.D. Pereira Netto, Optimization and application of methods of triacylglycerol evaluation for characterization of olive oil adulteration by soybean oil with HPLC–APCI-MS–MS, Talanta. 81 (2010) 1116–1125.
[40] M. Holčapek, P. Jandera, P. Zderadička, L. Hruba, Characterization of triacylglycerol and diacylglycerol composition of plant oils using high-performance liquid chromatography–atmospheric pressure chemical ionization mass spectrometry, J. Chromatogr. A. 1010 (2003) 195–215.
[41] F.S. Deschamps, P. Chaminade, D. Ferrier, A. Baillet, Assessment of the retention properties of poly(vinyl alcohol) stationary phase for lipid class profiling in liquid chromatography, J. Chromatogr. A. 928 (2001) 127–137.
[42] L. Yao, S. Jung, 31P NMR Phospholipid Profiling of Soybean Emulsion Recovered from Aqueous Extraction, J. Agric. Food Chem. 58 (2010) 4866–4872.
[43] C.S. Ejsing, J.L. Sampaio, V. Surendranath, E. Duchoslav, K. Ekroos, R.W. Klemm, K. Simons, A. Shevchenko, Global analysis of the yeast lipidome by quantitative shotgun mass spectrometry, Proc. Natl. Acad. Sci. 106 (2009) 2136–2141.
[44] C. Klose, M.A. Surma, M.J. Gerl, F. Meyenhofer, A. Shevchenko, K. Simons, Flexibility of a Eukaryotic Lipidome – Insights from Yeast Lipidomics, PLoS ONE. 7 (2012) e35063.
[45] S. Khoomrung, P. Chumnanpuen, S. Jansa-Ard, M. Ståhlman, I. Nookaew, J. Borén, J. Nielsen, Rapid Quantification of Yeast Lipid using Microwave-Assisted Total Lipid Extraction and HPLC-CAD, Anal. Chem. 85 (2013) 4912–4919.
[46] L. Imbert, R.G. Ramos, D. Libong, S. Abreu, P.M. Loiseau, P. Chaminade, Identification of phospholipid species affected by miltefosine action in Leishmania donovani cultures using LC-ELSD, LC-ESI/MS, and multivariate data analysis, Anal. Bioanal. Chem. 402 (2012) 1169–1182.
[47] L. Lindberg, A.X. Santos, H. Riezman, L. Olsson, M. Bettiga, Lipidomic Profiling of Saccharomyces cerevisiae and Zygosaccharomyces bailii Reveals Critical Changes in Lipid Composition in Response to Acetic Acid Stress, PLoS ONE. 8 (2013) e73936.
[48] C.S. Ejsing, T. Moehring, U. Bahr, E. Duchoslav, M. Karas, K. Simons, A. Shevchenko, Collision-induced dissociation pathways of yeast sphingolipids and their molecular profiling in total lipid extracts: a study by quadrupole TOF and linear ion trap–orbitrap mass spectrometry, J. Mass Spectrom. 41 (2006) 372–389.
[49] W. Xu, S. Yang, J. Zhao, T. Su, L. Zhao, J. Liu, Improving coenzyme Q8 production in Escherichia coli employing multiple strategies, J. Ind. Microbiol. Biotechnol. 41 (2014) 1297–1303.
[50] A. Laganowsky, E. Reading, T.M. Allison, M.B. Ulmschneider, M.T. Degiacomi, A.J. Baldwin, C.V. Robinson, Membrane proteins bind lipids selectively to modulate their structure and function, Nature. 510 (2014) 172–175.
[51] D. Oursel, C. Loutelier-Bourhis, N. Orange, S. Chevalier, V. Norris, C.M. Lange, Lipid composition of membranes of Escherichia coli by liquid chromatography/tandem mass spectrometry using negative electrospray ionization, Rapid Commun. Mass Spectrom. 21 (2007) 1721–1728.
[52] J. Gidden, J. Denson, R. Liyanage, D.M. Ivey, J.O. Lay, Lipid Compositions in Escherichia coli and Bacillus subtilis During Growth as Determined by MALDI-TOF and TOF/TOF Mass Spectrometry, Int. J. Mass Spectrom. 283 (2009) 178–184.

Table 1. Information about the lipid species composition of standards.
SQ-squalene, CE-cholesteryl esters, FAME-fatty acids methylesters, TG-triacylglycerols, Chol-cholesterol, DG-diacylglycerols, FA-fatty acids, MG-monoacylglycerols, Ceramides (CerII (Cer(d18:1/18:0)), CerIIIb (Cer(t18:0/18:1)), CerV (Cer(d18:1/18:0(2OH)) and CerVI (Cer(t18:0/18:0(2OH)))), ASG-acylated steryl glycosides, MGDG-monogalactosyldiglycerols, SG-steryl glycosides, GlcCer-glucosylceramides, DGDG-digalactosyldiglycerols, NAPE-N-Acylphosphatidylethanolamines, PG-phosphatidylglycerols, PE-phosphatidylethanolamines, PA-phosphatidic acids, PI-phosphatidylinositols, CL-cardiolipins, PS-phosphatidylserines, PC-phosphatidylcholines, SM-sphingomyelins, LPC-lysophosphatidylcholines.

A

Monomolecular lipids standards

Lipid Class	Isoprenoids	ST	FA	TG	DG	MG	Cer
Subclasses (species)	SQ	CE(16:0)	FAME(methyl-nonadecanoic acids)	TG (18:0/18:0/18:0)	DG (18:2/0:0/18:2)	MG (18:0/0:0/0:0)	Cer(d18 :1/18 :0)
		Chol	FA(18:0)		DG (16:0/16:0/0:0)		Cer(t18 :0/18 :1)
		ASG (18:2-Glc-Sitosterol)					Cer(d18 :1/18 :0(2OH))
							Cer(t18:0/18 :0(2OH))

B

Composition of natural PL standards (typical composition provided by Avanti Polar)

Lipid Class	PG	PE	PA	PI	CL	PS	PC	SM	LPC
FA%\origin	egg yolk chicken	egg yolk chicken	egg yolk chicken	bovine liver	bovine heart	bovine brain	egg yolk chicken	egg yolk chicken	egg yolk chicken
16:0	32.9	17.3	34.2				32.7	86	69
18:0	12.2	24.2	11.5	46		42	12.3	6	24.6
18:1	30.2	18.1	31.5	8	5	30	32		3.4
18:2	18.7	14	18.5	6	90		17.1		0.3
20:3				13					
20:4	3.5	16	2.7	17		2	2.7		
22:6		4.2				11			

C

Natural lipids standards (typical composition provided by Avanti Polar)

Lipid Class	DGDG	MGDG	Neutral glycosphingolipids
FA\origin	plant	plant	wheat
18:3-18:3	44.5	14.1	GlcCer(d18:2/16:0(OH))
18:2-18:3	10.7	3.2	GlcCer(d18:1/16:0(OH))
16.3-18:3	21.3	66.8	GlcCer(d18:1/20:0(OH))
16:3-18:2	7	12.9	
16:1-18:3	6.9	3	
16:0-18:3	9.7		

D

Other subclasses of lipids found in samples

Lipid Class	Quinones and hydroquinones	ST	Neutral glycosphingolipids	PE
origin	brain	Wheat	brain	Wheat
Subclasses	coenzyme Q10	SG	HexCer	NAPE
			HexCer(OH)	

Table 2. Quaternary gradient mobile phase composition. A, isooctane:ethyl acetate (99.8:0.2, v/v); B, acetone:ethyl acetate (2:1, v/v) containing 0.15% acetic acid (v/v); C, 2-propanol:water (85:15, v/v) containing 0.043% acetic acid (v/v) and 0.104% trimethylamine (v/v); D, ethyl acetate.

Time (min)	Percent solvent				Flow-rate (mL/min)
	A	B	C	D	
0	100	0	0	0	0.8
1.5	100	0	0	0	0.8
1.6	97	3	0	0	0.8
9	94	6	0	0	0.8
11	70	30	0	0	0.8
14	45	55	0	0	0.8
15	45	55	0	0	0.8
16	40	55	5	0	0.8
20	35	55	10	0	0.8
20.1	33	50	17	0	0.8
25	38	45	17	0	0.8
25.1	48	35	17	0	0.8
30	53	30	17	0	0.8
40	40	0	60	0	0.8
40.1	0	100	0	0	0.8
42	0	100	0	0	0.8
42.1	50	0	0	50	0.8
45	50	0	0	50	0.8
47	100	0	0	0	0.8
53	100	0	0	0	0.8

Table 3. Changes and evolution of the lipid class analysis method from Christie to this work. Abbreviation: acetic acid (AA), 2-propanol (IPA), ethanolamine (EA), trimethylamine (TEA), tetrahydrofuran (THF). The full name of lipids can be retrieved in table S-1.
SQ-squalene, SE-sterol ester, CE-cholesteryl esters, FAME-fatty acids methylesters, DGE- diacylglycerol ethers, TG-triacylglycerols, Chol-cholesterol, DG-diacylglycerols, FA-fatty acids, FAlc- fatty acids alcohol, MG-monoacylglycerols, ceramides (CerII (Cer(d18:1/18:0)), CerIIIb (Cer(t18:0/18:1)), CerV (Cer(d18:1/18:0(2OH)) and CerVI (Cer(t18:0/18:0(2OH)))), ASG-acylated steryl glycosides, MGDG-monogalactosyldiglycerols, SG-steryl glycosides, GlcCer-glucosylceramides, HexCER- hexosylceramide, DGDG-digalactosyldiglycerols, NAPE-N-Acylphosphatidylethanolamines, PG-phosphatidylglycerols, DPG- diphosphatidylglycerol, PE-phosphatidylethanolamines, PA-phosphatidic acids, PI-phosphatidylinositols, CL-cardiolipins, PS-phosphatidylserines, PC-phosphatidylcholines, SM-sphingomyelins, LPC-lysophosphatidylcholines.

Author (year)	Christie [10] (1985)	Homan [13] (1998)	Graeve [11] (2009)	Gerits [12] (2013)	McLaren [9] (2011)	Present study (2017)
Column	Spherisorb 3µm Si 100 X 5 mm	Spherisorb 5µm Si 100 X 4.6 mm	Chromolith Si 100 X 4.6 mm	Chromolith Si 100 X 4.6 mm	Halo HILIC 2.7 µm 50 X 2.1 mm	Inertsil 5µm Si 150 X 2.1 mm
Temperature		45°C	40°C	40°C		40°C
Analysis time	30 min	30 min	35 min	35 min	10.5 min	53 min
Flow rate	2 ml/min	1.6 - 2 ml/min	1.4 – 3 ml/min	1.4 – 3 ml/min	1.2 ml/min	0.8 ml/ min
injected Volume	5 µl	10 µl	2 – 60 µl	1 – 50 µl	2 µl	2 µl
injection Solvent	Chloroform:isooctane (1:1, v/v)	Isooctane:THF (9:1, v/v)	Isooctane:ethyl acetate (9:1, v/v) or Dichloromethane:methanol (2:1, v/v)	Isooctane	Isooctane:THF:methanol (9:1:1, v/v/v)	Isooctane:chloroform (4:1, v/v)
Detector	ELSD	ELSD	ELSD	ELSD	ELSD	ELSD / CAD / ESI / APCI / APPI
Solvent A	Isooctane:THF (99:1, v/v)	Isooctane:THF (99:1, v/v)	Isooctane:ethyl acetate (99.8:0.2, v/v)	Isooctane	Isooctane:THF (99:1, v/v)	Isooctane:ethyl acetate (99.8:0.2, v/v) pressurized
Solvent B	IPA:chloroform (4:1, v/v)	Acetone:dichnloromethane (2:1, v/v)	Acetone:ethyl acetate (2:1, v/v) + AA (0.02% (v/v))	Acetone:ethyl acetate (2:1, v/v) + 70 mM AA	Acetone:dichnloromethane (4:1, v/v)	Acetone:ethyl acetate (2:1, v/v) + 35 mM AA
Solvent C	IPA:water (1:1, v/v)	IPA:water (85:15, v/v) + 7.5 mM AA + 7.5mM EA	IPA:water (85:15, v/v) + 7.5 mM AA + 7.5mM EA	IPA:water (85:15, v/v) + 7.5 mM AA + 7.5mM TEA	IPA:chloroform (80:20, v/v)	IPA:water (85:15, v/v) + 7.5 mM AA + 7.5mM TEA
Solvent D				IPA	IPA:water (1:1, v/v)	Ethyl acetate
Samples investigated	heart, erythrocytes, plasma	heart, liver, brain, Kidney	marine zooplankton	wheat	plasma, liver, heart	heart, liver, brain, yeast, *E. coli*, soy, wheat
Standards used to optimize the analytical method	CE, TG, Chol, DG, FA, DPG, PE, PI, PS, PC, SM, LPC	CE, TG, Chol, DG, FA, MG, HexCer, HexCer(OH), CL, PE, PI, PS, PC, SM, LPC	SQ, SE, WE, FAME, DGE, TG, FAlc, ST, DG, FA, HexCer, CL, PE, PI, PS, PC, LPC	TG, Chol, DG, FA, MG, MGDG, DGDG, NAPE, PE, PA, PG, NALPE, PI, PC, LPC	CE, TG, FA, Chol, DG, PE, PC	SQ, CE, FAME, TG, Chol, DG, FA, MG, CerII, CerIII, CerV, CerVI, ASG, MGDG, GlcCer, DGDG, PG, PE, PA, PI, CL, PS, SM, LPC
Lipids classes and subclasses identified in samples	CE, TG, Chol, DG, FA, DPG, PE, PI, PS, PC, SM, LPC	CE, TG, Chol, HexCer, HexCer(OH), CL,PE, PI, PS, PC, SM	Sql, WE, DGE, TG, FAlc, ST, FA, HexCer, CL, PE, PI, PS, PC, LPC	TG, Chol, DG, FA, MG, MGDG, DGDG, NAPE, PE, NALPE, PI, PC, LPC	CE, TG, FA, Chol, PE, PC, CL	SQ, SE, Coenzyme, TG, ST, Chol, DG, FA, MG, Cer, ASG, MDGD,SG, GlcCer, HexCer, HerCer(OH), DGDG, NAPE, PG, PE, PA, PI, CL, PS, PC, SM, LPC

Table 4. APPI negative and positive mode: characteristics ions of some lipid species encountered in lipid standards and samples (see text for details). A retention time noted x-y indicates a broad peak and x;y indicates a dual peak. Ions between brackets have an intensity of less than 5.10^6 counts. For PL, the FA indication is not positional.
SQ-squalene, CE-cholesteryl esters, FAME-fatty acids methylesters, TG-triacylglycerols, Chol-cholesterol, DG-diacylglycerols, FA-fatty acids, MG-monoacylglycerols, Ceramides (CerII (Cer(d18:1/18:0)), CerIIIb (Cer(t18:0/18:1)), CerV (Cer(d18:1/18:0(2OH)) and CerVI (Cer(t18:0/18:0(2OH)))), ASG-acylated steryl glycosides, MGDG-monogalactosyldiglycerols, SG-steryl glycosides, GlcCer-glucosylceramides, DGDG-digalactosyldiglycerols, NAPE-N-Acylphosphatidylethanolamines, PG-phosphatidylglycerols, PE-phosphatidylethanolamines, PA-phosphatidic acids, PI-phosphatidylinositols, CL-cardiolipins, PS-phosphatidylserines, PC-phosphatidylcholines, SM-sphingomyelins, LPC-lysophosphatidylcholines.

Lipid species	Rt. (min)	Molecular mass (g/mol)	APPI -					APPI +					
			$[M-H]^-$	$[M-CH3]^-$	$[M^\circ]^-$	$[M-H+CH_3COOH]^-$	$[FA-H]^-$	$[M+H]^+$	$[M + Na]^+$	$[M+H-FA]^+$			
SQ	0.7	410.4	(409.4)					411.4					
CE(16:0)	1.7-2.8	624.6					(255.2)			369.4			
FAME(methyl-nonadecanoic acids)	2.5	312.3					(297.3)	(313.3)					
TG(18:0/18:0/18:0)	4.6	890.8	(889.8)				283.3			607.6			
Coenzyme Q10	4.6	862.7	(861.7)					(863.7)					
										$[M+H-H_2O]^+$	[M-FA-sugar+ H+H2O]$^+$	[Aglycone+ H-H2O]$^+$	[Aglycone +H]$^+$
Chol	7.4	386.4								(369.4)			
DG(18:2/0:0/18:2)	9.3	616.5	(615.5)			(675.5)	279.2	617.5		599.5			
DG(16:0/16:0/0:0)	10.4	568.5				(627.5)	255.2			551.5			
FA(18:0)	11.4	284.3	283.3				283.3						
Cer II : Cer(d18:1/18 :0)	13.4; 13.7	567.6	566.6			626.6		568.7		550.7			
Cer IIIb : Cer(t18:0/18 :1)	14.2	583.6	582.5			642.6		584.6		566.6			
Cer V : Cer(d18:1/18 :0(2OH))	14.0; 14.9	581.5	580.6			(640.5)				564.6			
Cer VI : Cer(t18:0/18 :0(2OH))	14.5; 15.8	599.5	598.5			(658.5)		600.6		582.5			
MG(18:0/0:0/0:0)	13	358.3				(417.3)	(283.3)	(359.3)		(341.3)			
ASG(18:2-Glc-Sitosterol)	14.5	838.7				897.7	279.2				397.3		
MGDG(18:3/16:3)	17	746.5	745.5			805.5	249.2 / 277.2		769.5			585.5	
SG(Sitosteryl glucoside)	17.6	576.4				(635.5)						(397.3)	
GlcCer(d18:2/20:0(OH))	19.5	771.6	770.6						(794.6)			(610.6)	
HexCer	19	809.7	808.8							792.8			
HexCer(OH)	19.5	827.7	826.8							810.8			
DGDG(18:3/18:3)	21.8	936.6	935.6			995.6	(277.2)		(959.6)				(613.4)
										$[M+H-polar\ Head]^+$		**Diglyceride like ion**	
NAPE(18:2-16:0-N18:2)	24.4	977.7	(976.7)				(255.2)/(297.3)		(1000.7)			(575.6)	
PG(16:0_18:1)	28.7	748.5	747.5				(255.2)/(281.2)		771.5	$[M+H-172]^+$=	577.5		
PE(18:2_18:0)	29.5	743.5	742.5				(279.2)/(283.3)		(766.5)	$[M+H-141]^+$=	(603.5)		
PA(16:0_18:1)	30.7	674.5	673.5				(255.2)/(281.2)		(697.5)	$[M+H-98]^+$=	577.5		
PI(18:0_20:4)	33	886.6	885.5				(283.3)/(303.2)		(909.5)	$[M+H-260]^+$=	627.6		
CL([18:2/18:2],-[18:2/18:2])	34	1449.0	1448.0				279.2		1472.0			599.6	
PS(18:0_18:1)	34.6	789.6	788.5				(280.2)/(283.3)		812.5	$[M+H-185]^+$=	605.7		
PC(16:0_18:1)	35.3	759.6		744.6	759.6		(255.2)/(281.2)	(760.6)		$[M+H-183]^+$=	577.5		
SM(d18:1/16:0)	36.4	702.6		687.5	(702.6)			(703.6)		$[M+H-183]^+$=	(520.5)		
LPC(0 :0/18 :0)	38.9	523.4		(508.4)	(523.4)		283.3	(524.4)					
LPC(16:0/0 :0)	39.6	495.3		(480.3)	(495.3)		(255.2)	(496.3)					

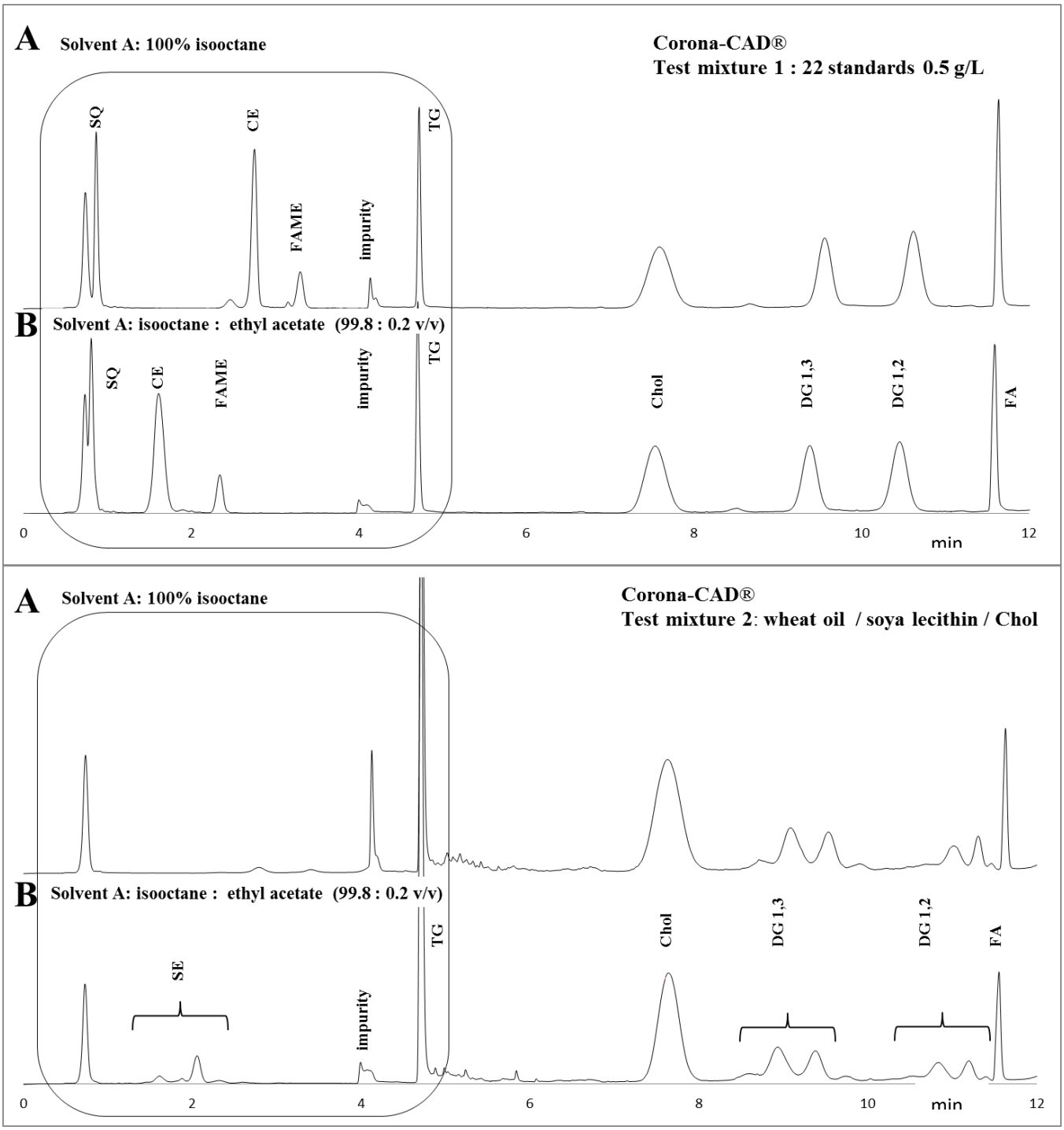

Figure 1. Influence of the initial mobile phase composition on the first part of the chromatogram (0~12 min) for test mixtures 1 (top) and 2 (bottom). (A) 100% isooctane (B) isooctane:ethyl acetate (99.8:0.2, v/v). The other mobiles phases of the solvent program are as indicated in table 2. SQ-squalene, SE-sterol ester, CE-cholesteryl esters, FAME-fatty acids methylesters, TG-triacylglycerols, ST-sterols, Chol-cholesterol, DG-diacylglycerols, FA-fatty acids. Detector: Corona-CAD®.

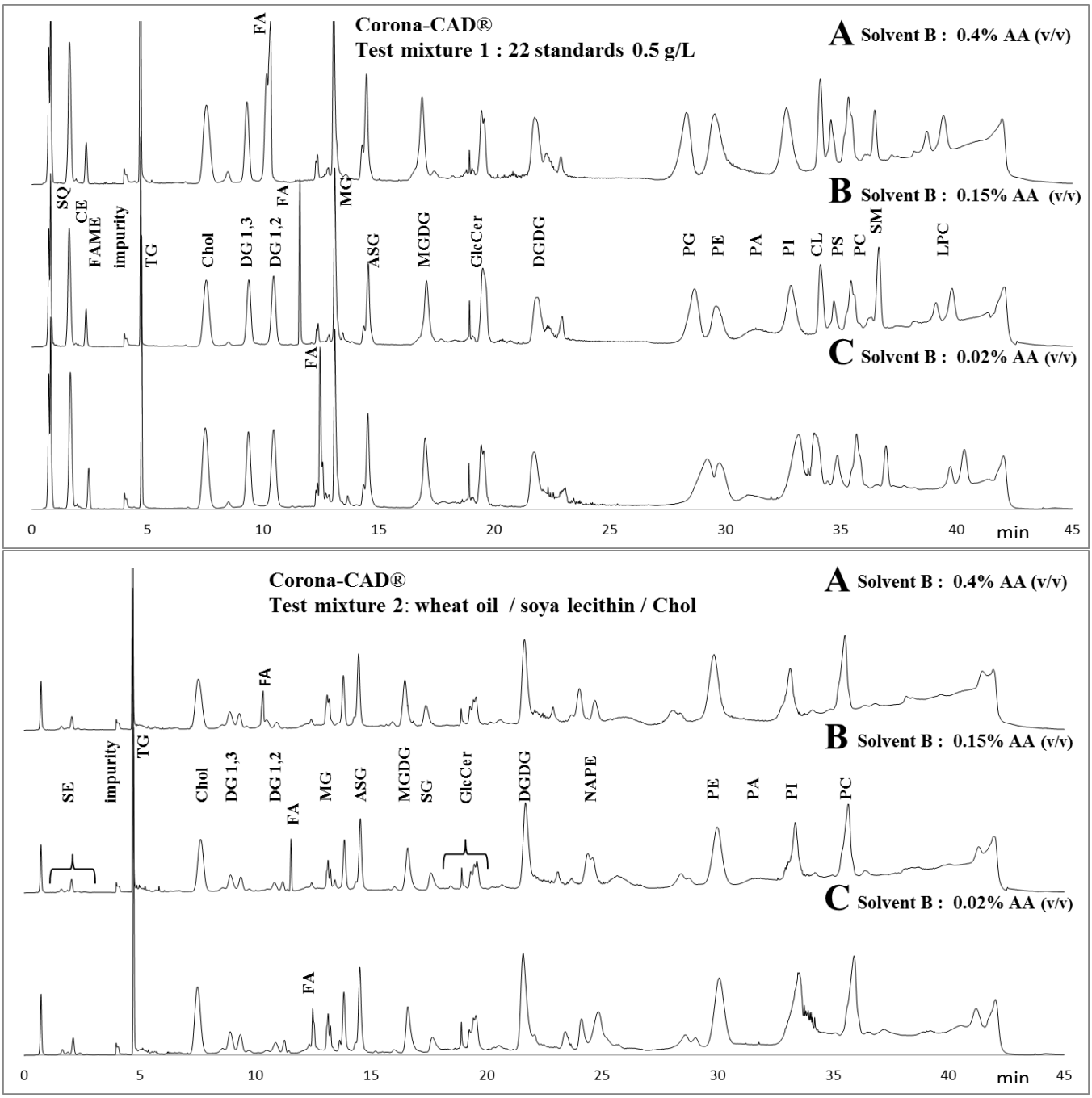

Figure 2. Influence of the amount of acetic acid in the B phase of the solvent program on the chromatogram of test mixtures 1 (top) and 2 (bottom). (A) 0.4 %, (B) 0.15 % (C) 0.02 % acetic acid (v/v) in acetone:ethyl acetate (2: 1, v/v). The other mobiles phases of the solvent program are as indicated in table 2. SQ-squalene, SE-sterol ester, CE-cholesteryl esters, FAME-fatty acids methylesters, TG-triacylglycerols, Chol-cholesterol, DG-diacylglycerols, FA-fatty acids, MG-monoacylglycerols, ASG-acylated steryl glycosides, MGDG-monogalactosyldiglycerols, SG-steryl glycosides, GlcCer-glucosylceramides, DGDG-digalactosyldiglycerols, NAPE-N-Acylphosphatidylethanolamines, PG-

phosphatidylglycerols, PE-phosphatidylethanolamines, PA-phosphatidic acids, PI-phosphatidylinositols, CL-cardiolipins, PS-phosphatidylserines, PC-phosphatidylcholines, SM-sphingomyelins, LPC-lysophosphatidylcholines. Detector: Corona-CAD®.

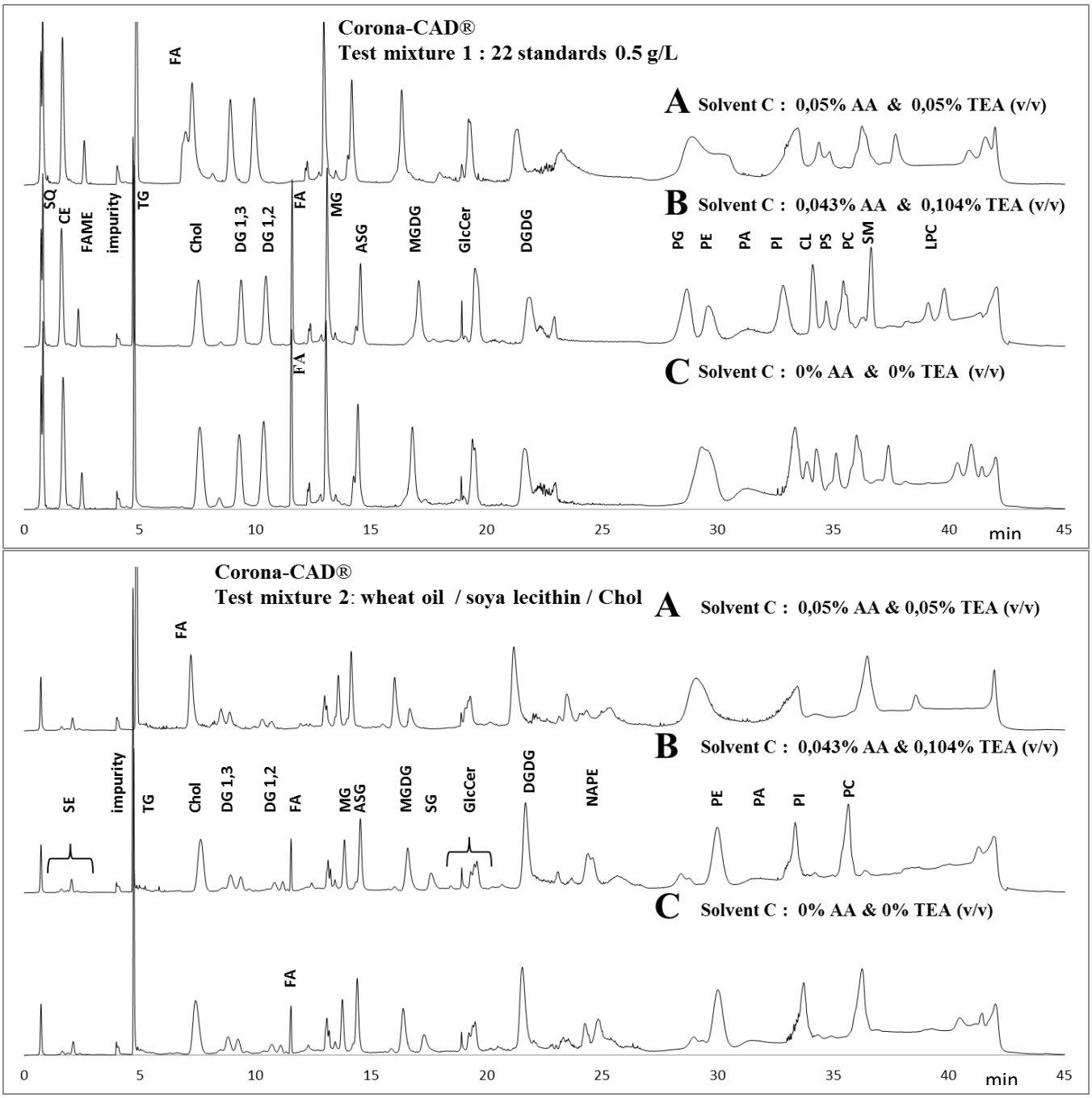

Figure 3. Influence of the amounts of acetic acid and trimethylamine in the C phase of the solvent program on the chromatogram of test mixtures 1 (top) and 2 (bottom). (A) 0.05% AA & TEA (v/v), (B) 7.5mM AA & TEA (0.043% AA & 0.104% TEA) and (C) without AA or TEA. The other mobiles phases of the solvent program are as indicated in table 2. SQ-squalene, SE-sterol ester, CE-cholesteryl esters, FAME-fatty acids methylesters, TG-triacylglycerols, Chol-cholesterol, DG-diacylglycerols, FA-fatty acids, MG-monoacylglycerols, ASG-acylated steryl glycosides, MGDG-monogalactosyldiglycerols, SG-steryl glycosides, GlcCer-glucosylceramides, DGDG-digalactosyldiglycerols, NAPE-N-

Acylphosphatidylethanolamines, PG-phosphatidylglycerols, PE-phosphatidylethanolamines, PA-phosphatidic acids, PI-phosphatidylinositols, CL-cardiolipins, PS-phosphatidylserines, PC-phosphatidylcholines, SM-sphingomyelins, LPC-lysophosphatidylcholines. Detector: Corona-CAD®.

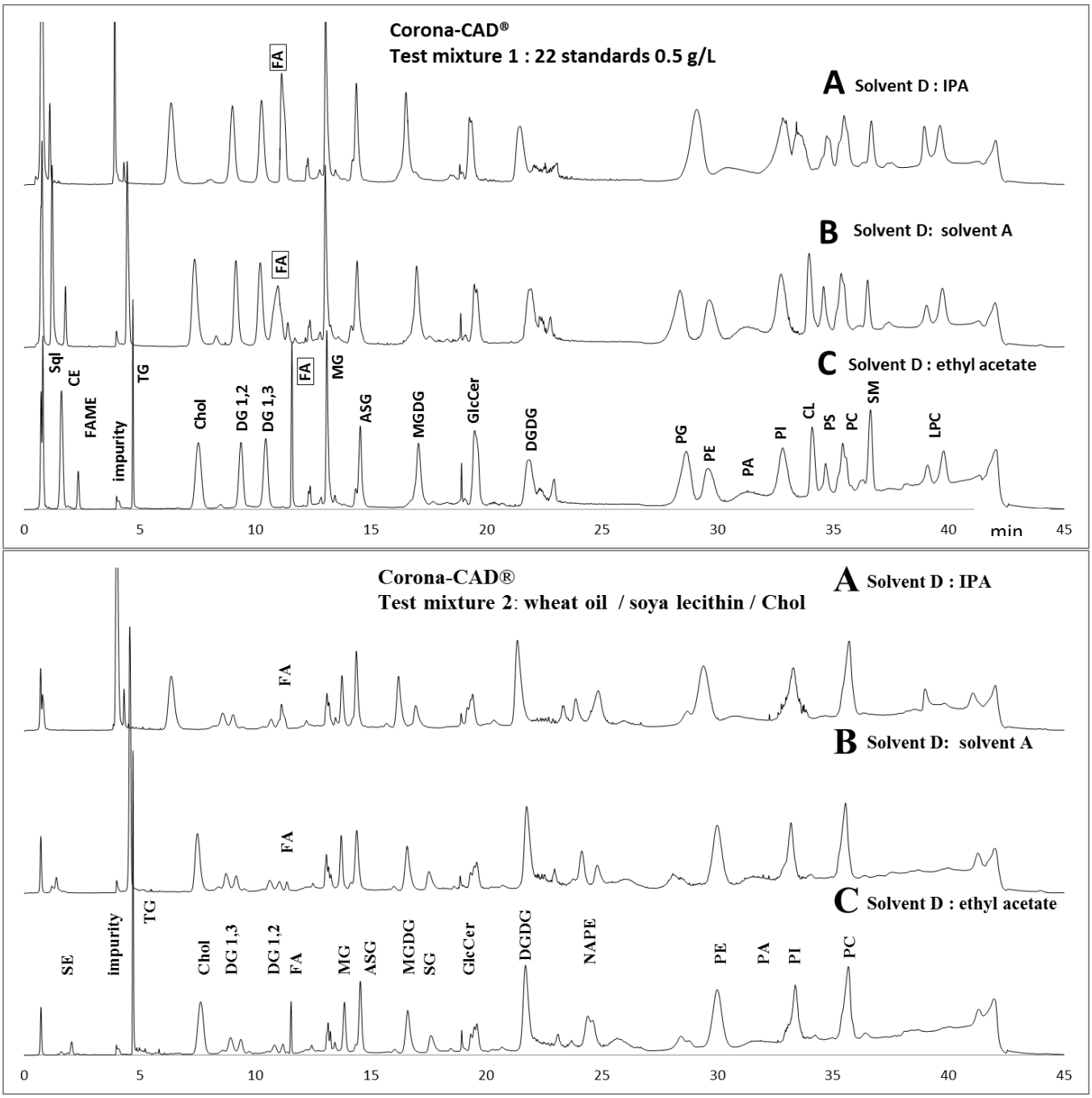

Figure 4. Influence of the rinsing step (mobile phase D) on the chromatogram of test mixture 1 (top) and 2 (bottom): (A) isopropanol (B) isooctane: ethyl acetate (99.8: 0.2, v/v) (C) ethyl acetate (C). The other mobiles phases of the solvent program are as indicated in table 2. SQ-squalene, SE-sterol ester, CE-cholesteryl esters, FAME-fatty acids methylesters, TG-triacylglycerols, Chol-cholesterol, DG-diacylglycerols, FA-fatty acids, MG-monoacylglycerols, ASG-acylated steryl glycosides, MGDG-monogalactosyldiglycerols, SG-steryl glycosides, GlcCer-glucosylceramides, DGDG-digalactosyldiglycerols, NAPE-N-

Acylphosphatidylethanolamines, PG-phosphatidylglycerols, PE-phosphatidylethanolamines, PA-phosphatidic acids, PI-phosphatidylinositols, CL-cardiolipins, PS-phosphatidylserines, PC-phosphatidylcholines, SM-sphingomyelins, LPC-lysophosphatidylcholines. Detector: Corona-CAD®.

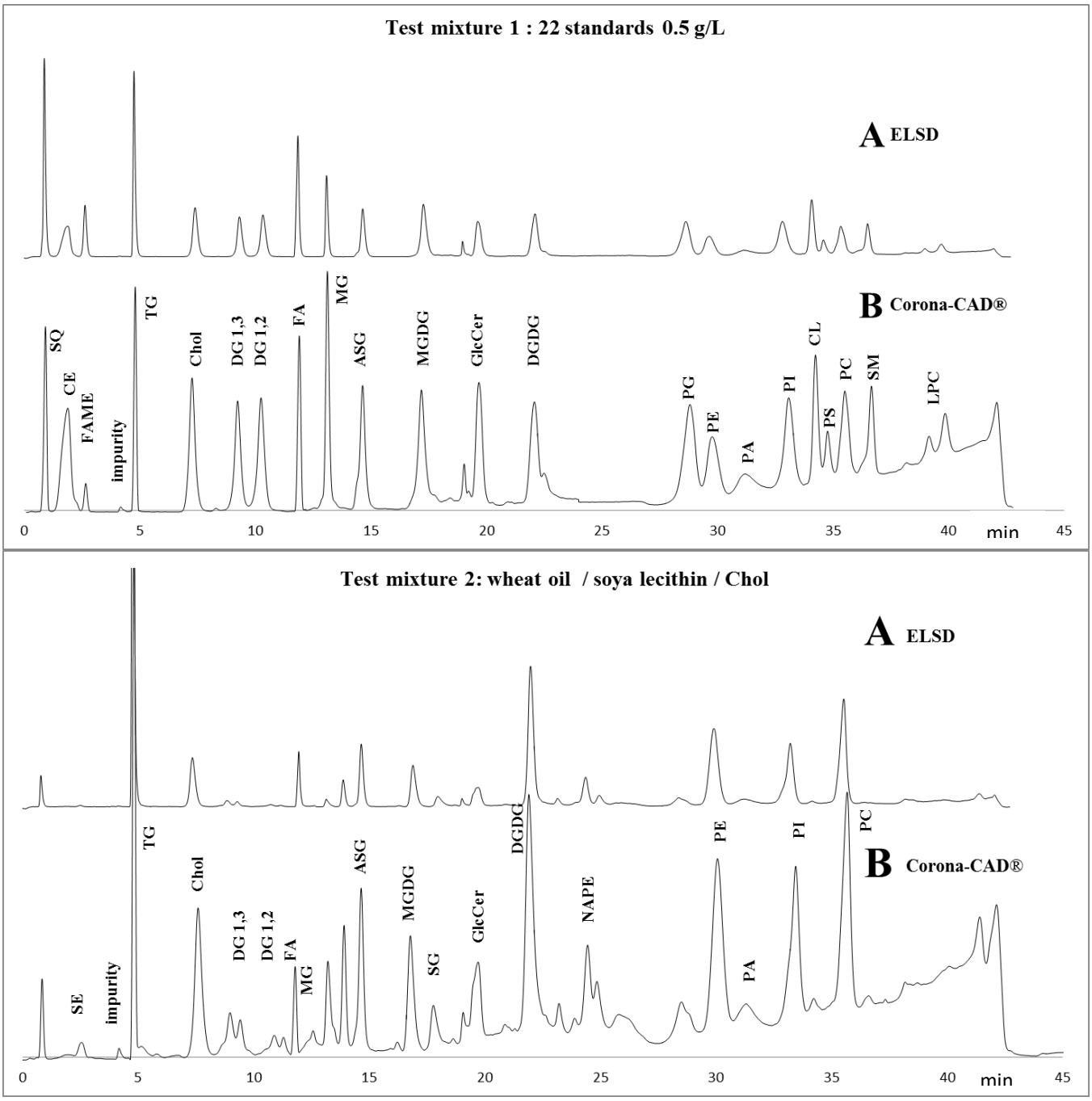

Figure 5. Chromatographic profiles of test mixtures 1 (top) and 2 (bottom) obtained with (A) ELSD and (B) Corona-CAD® detection. SQ-squalene, SE-sterol ester, CE-cholesteryl esters, FAME-fatty acids methylesters, TG-triacylglycerols, Chol-cholesterol, DG-diacylglycerols, FA-fatty acids, MG-monoacylglycerols, ASG-acylated steryl glycosides, MGDG-monogalactosyldiglycerols, SG-steryl glycosides, GlcCer-glucosylceramides, DGDG-digalactosyldiglycerols, NAPE-N-Acylphosphatidylethanolamines, PG-phosphatidylglycerols, PE-phosphatidylethanolamines, PA-phosphatidic acids, PI-

phosphatidylinositols, CL-cardiolipins, PS-phosphatidylserines, PC-phosphatidylcholines, SM-sphingomyelins, LPC-lysophosphatidylcholines. Detector: Corona-CAD®.

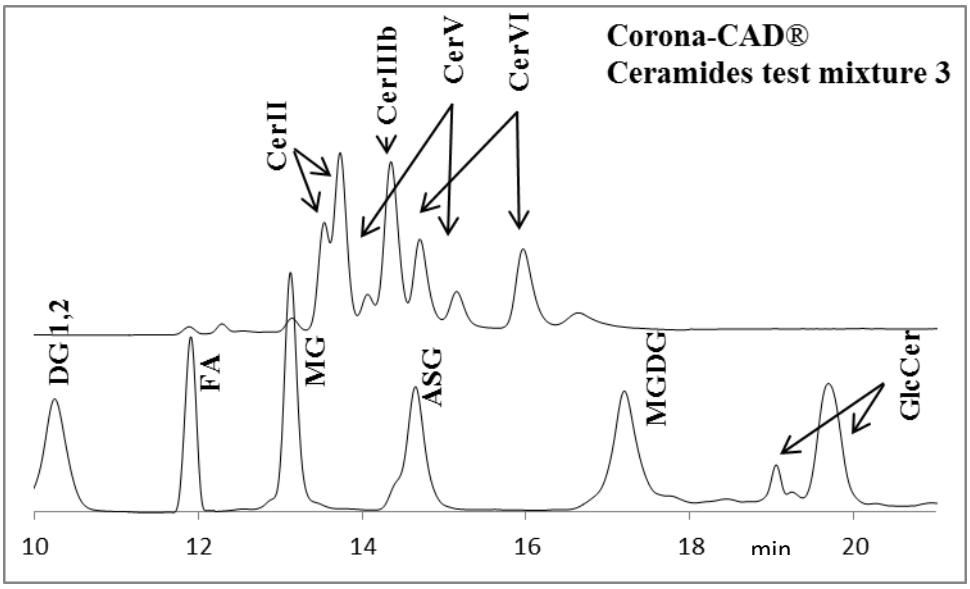

Figure 6. Superimposition of chromatographic profiles of ceramides subclasses (test mixture 3) and chromatographic profile of standards (test mixture 1) obtained with Corona-CAD®.

Ceramides (CerII (Cer(d18:1/18:0)), CerIIIb (Cer(t18:0/18:1)), CerV (Cer(d18:1/18:0(2OH)) and CerVI (Cer(t18:0/18:0(2OH)))), DG-diacylglycerols, FA-fatty acids, MG-monoacylglycerols, ASG-acylated steryl glycosides, MGDG-monogalactosyldiglycerols, SG-steryl glycosides, GlcCer-glucosylceramides. Detector: Corona-CAD®.

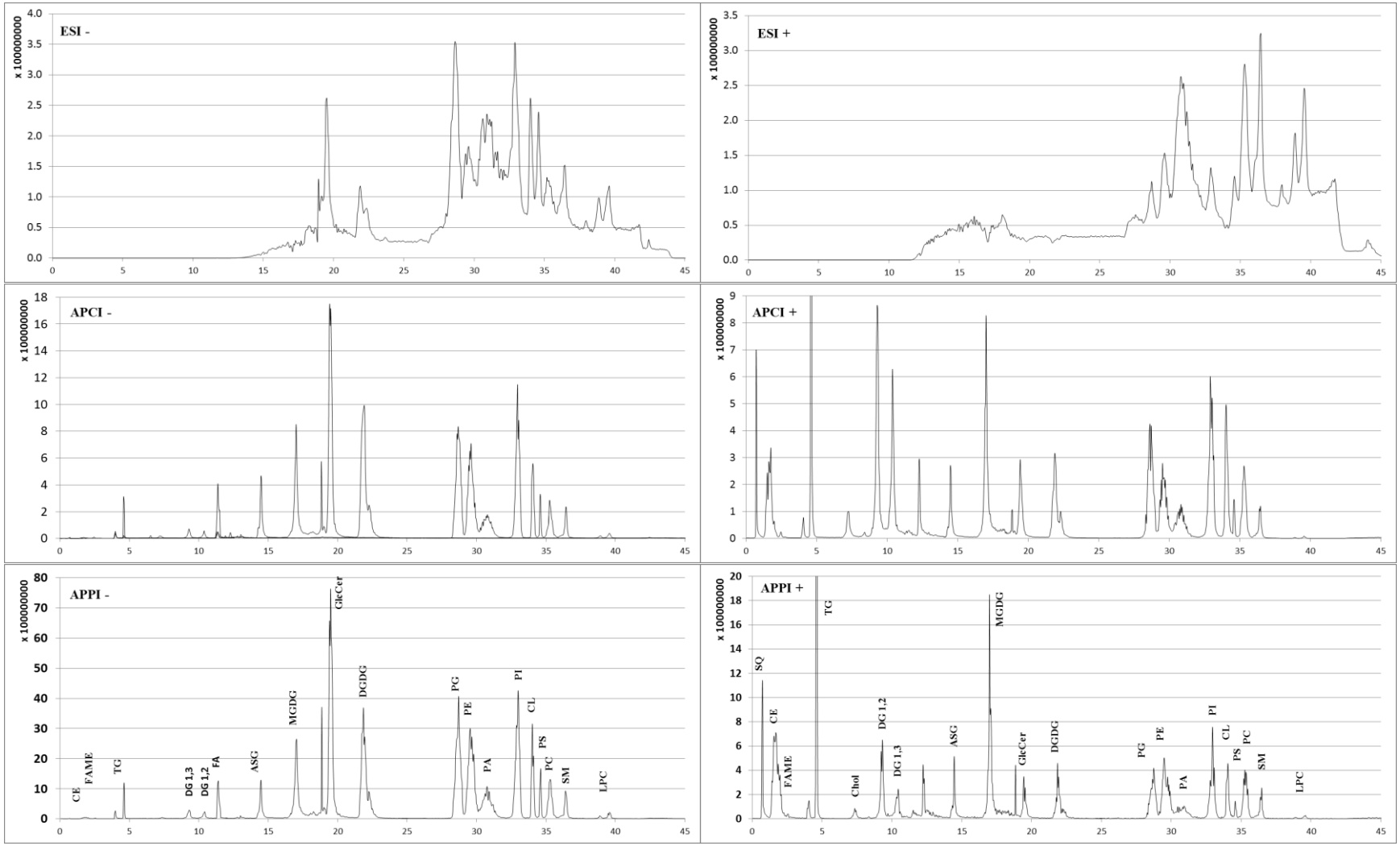

Figure 7. LC/MS chromatographic profile of mixture 1, using three different ion sources: ESI (top), APCI (middle) and APPI (down), in negative ion mode (left) and positive ion mode (right).

SQ-squalene, CE-cholesteryl esters, FAME-fatty acids methylesters, TG-triacylglycerols, Chol-cholesterol, DG-diacylglycerols, FA-fatty acids, ASG-acylated steryl glycosides, MGDG-monogalactosyldiglycerols, GlcCer-glucosylceramides, DGDG-digalactosyldiglycerols, PG-phosphatidylglycerols, PE-phosphatidylethanolamines, PA-phosphatidic acids, PI-phosphatidylinositols, CL-cardiolipins, PS-phosphatidylserines, PC-phosphatidylcholines, SM-sphingomyelins, LPC-lysophosphatidylcholines.

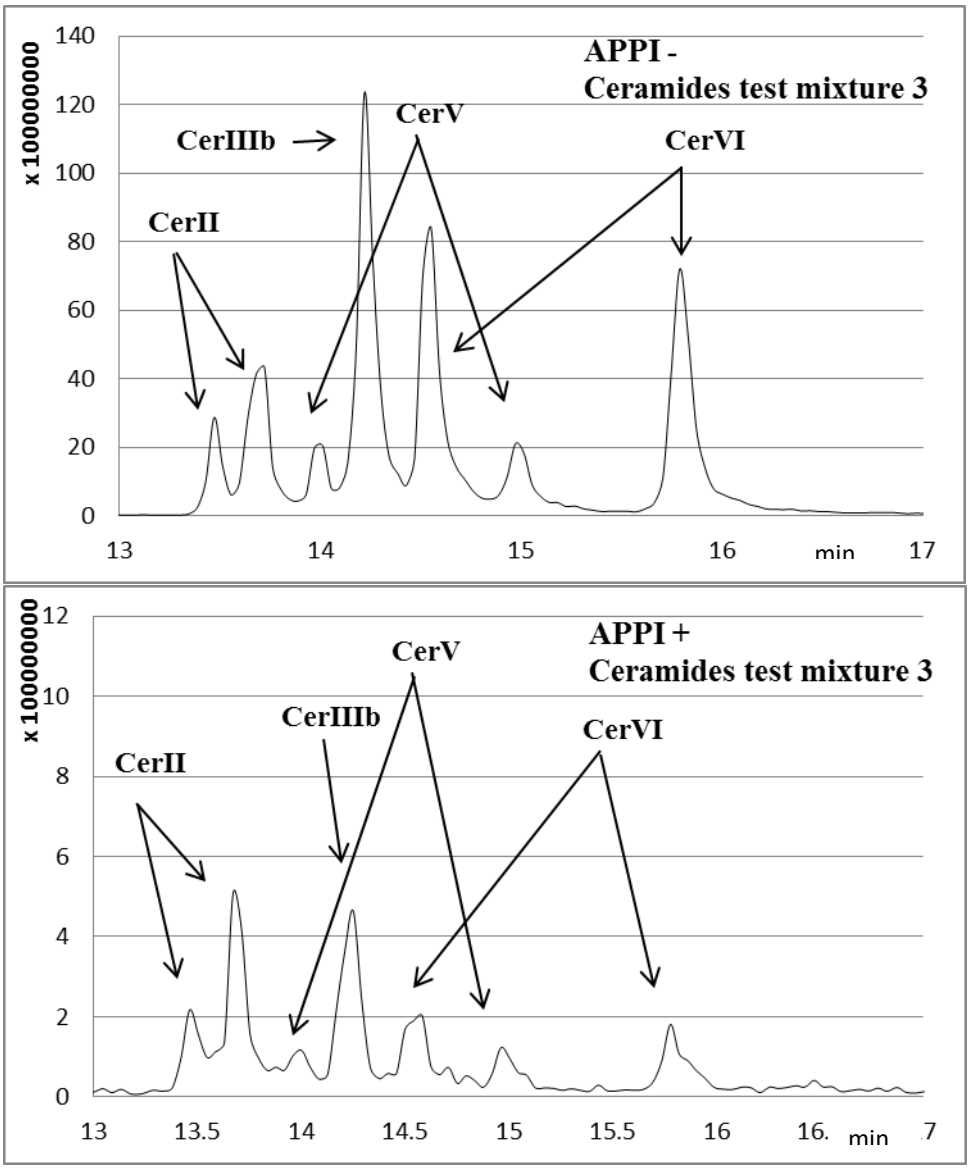

Figure 8. LC/MS chromatographic profile of test mixture 3, using APPI, in negative ion mode (top) and positive ion mode (down).

Ceramides (CerII (Cer(d18:1/18:0)), CerIIIb (Cer(t18:0/18:1)), CerV (Cer(d18:1/18:0(2OH)) and CerVI (Cer(t18:0/18:0(2OH)))).

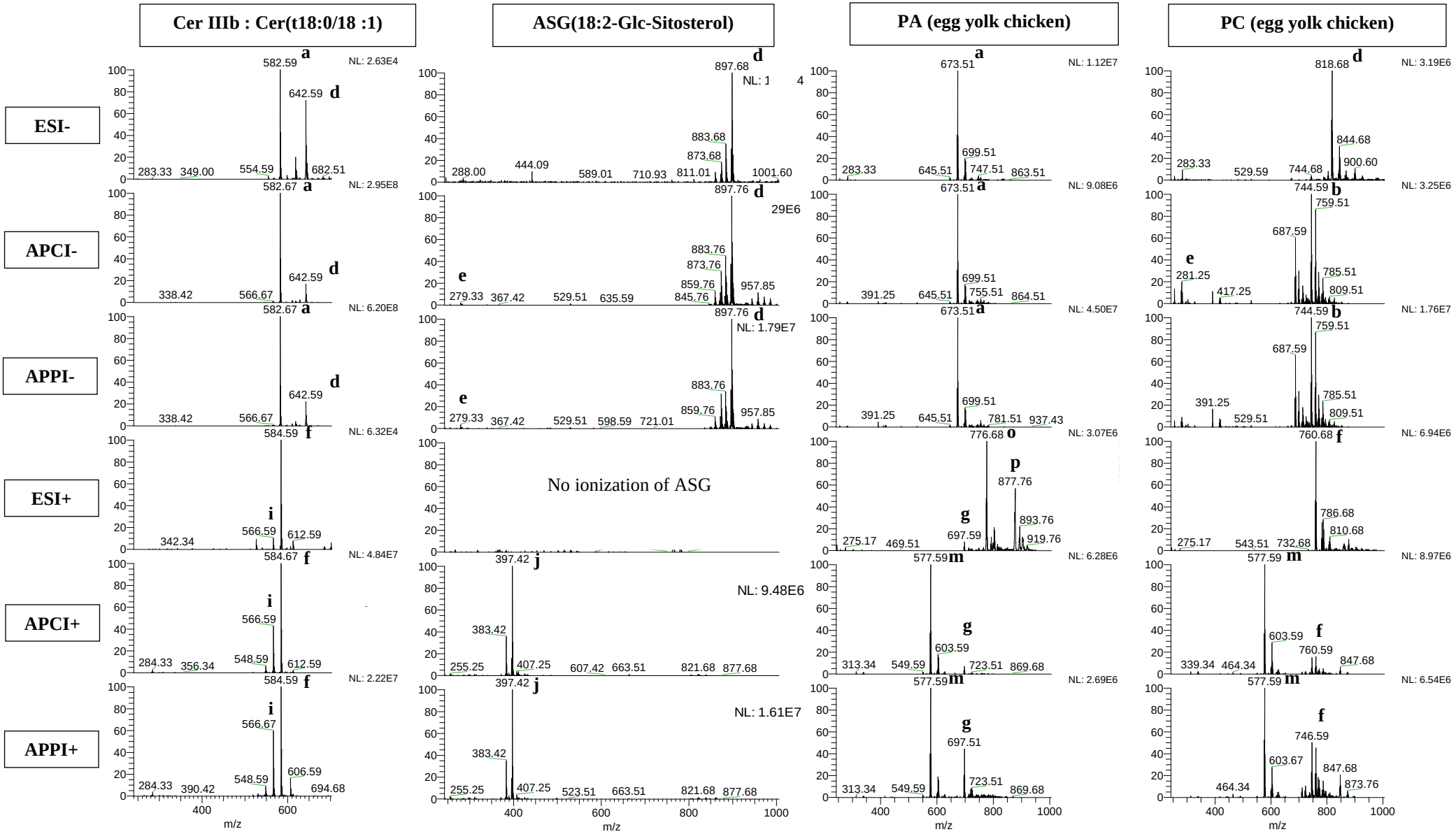

Figure 9. LC/MS full scan spectra obtained with the 3 API sources in positive and negative mode.

a : $[M-H]^-$, b : $[M-CH3]^-$, c : $[M°]^-$, d : $[M-H+CH_3COOH]^-$, e : $[FA-H]^-$, f : $[M+H]^+$, g : $[M + Na]^+$, h : $[M+H-FA]^+$, i : $[M+H-H_2O]^+$, j : $[M-FA-sugar+H+H2O]^+$, k : $[Aglycone+H-H2O]^+$, l : $[Aglycone+H]^+$, m : $[M+H-polar\ Head]^+$, n : Diglyceride like ion, o : $[M+H+TEA]^+$ and p : $[M+H+2TEA]^+$.

CerIIIb (Cer(t18:0/18:1)), ASG-acylated steryl glycosides, PA-phosphatidic acids, PC-phosphatidylcholines.

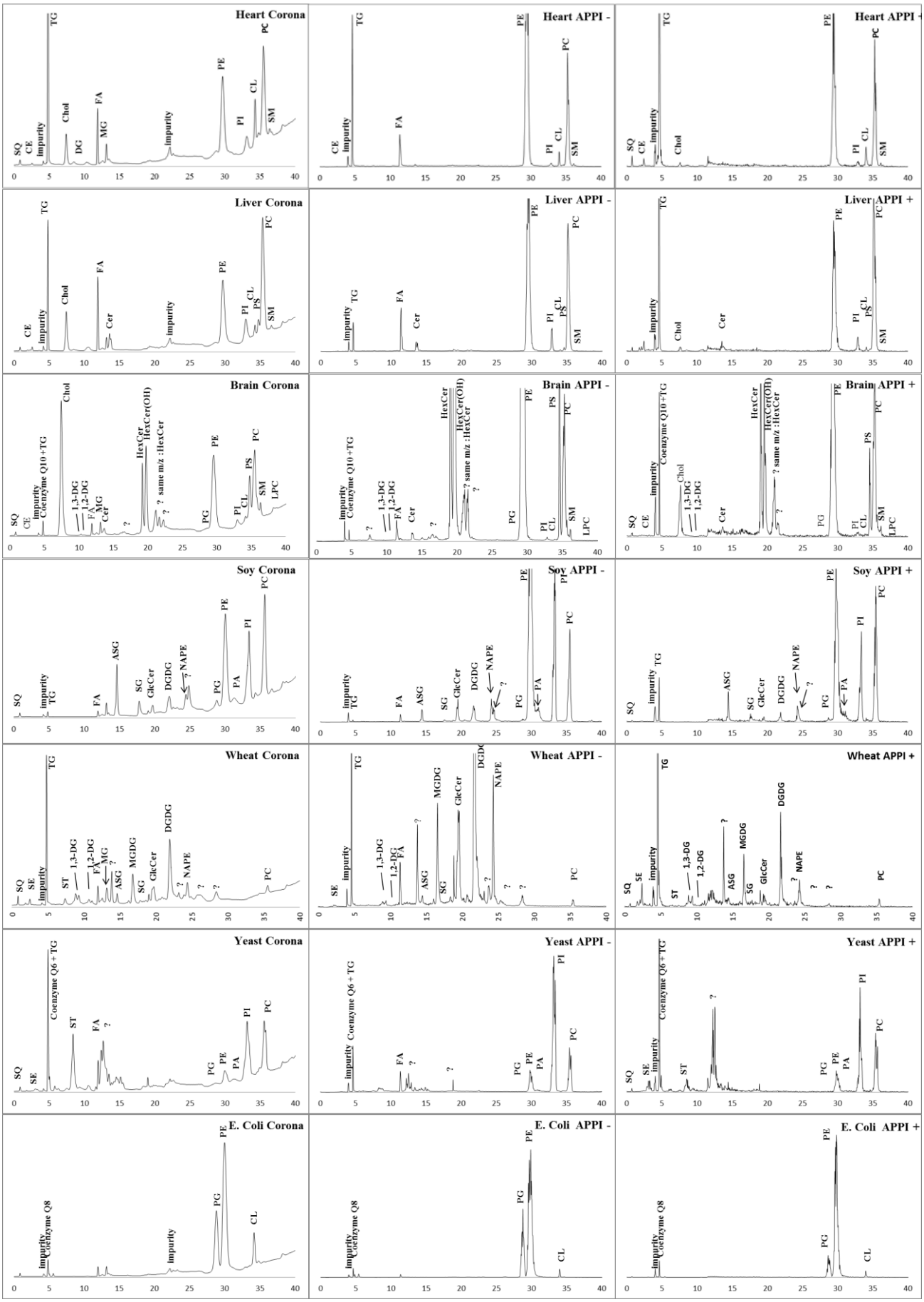
Heart Corona
SQ
CE
Impurity
TG
Chol
DG
FA
MG
Impurity
PE
PI
CL
SM
PC
Heart APPI -
CE
Impurity
TG
FA
PE
PI
CL
SM
PC
Heart APPI +
SQ
CE
Impurity
TG
Chol
PE
PI
CL
SM
PC
Liver Corona
CE
Impurity
TG
Chol
FA
Cer
Impurity
PE
PI
CL
PS
SM
PC
Liver APPI -
Impurity
TG
FA
Cer
PE
PI
CL
PS
SM
PC
Liver APPI +
Impurity
Chol
Cer
PE
PI
CL
PS
SM
PC
Brain Corona
SQ
CE
Impurity
Coenzyme Q10+TG
Chol
1,3-DG
1,2-DG
FA
MG
Cer
?
HexCer
HexCer(OH)
? same m/z :HexCer
?
PG
PE
PI
CL
PS
SM
PC
LPC
Brain APPI -
Impurity
Coenzyme Q10+TG
?
1,3-DG
1,2-DG
PA
Cer
?
HexCer
HexCer(OH)
? same m/z :HexCer
?
PG
PE
PS
PC
PI
CL
SM
LPC
Brain APPI +
SQ
CE
Impurity
Coenzyme Q10+TG
Chol
1,3-DG
1,2-DG
Cer
HexCer
HexCer(OH)
? same m/z :HexCer
?
PG
PE
PS
PC
PI
CL
SM
LPC
Soy Corona
SQ
Impurity
TG
FA
ASG
SG
GlcCer
DGDG
NAPE
?
PG
PA
PE
PI
PC
Soy APPI -
Impurity
TG
FA
ASG
SG
GlcCer
DGDG
NAPE
?
PG
PA
PE
PI
PC
Soy APPI +
SQ
Impurity
TG
ASG
SG
GlcCer
DGDG
NAPE
?
PG
PA
PE
PI
PC
Wheat Corona
SQ
SE
Impurity
TG
ST
1,3-DG
1,2-DG
FA
MG
?
ASG
MGDG
SG
GlcCer
DGDG
?
NAPE
?
?
PC
Wheat APPI -
SE
Impurity
TG
1,3-DG
1,2-DG
FA
?
ASG
MGDG
SG
GlcCer
DGDG
NAPE
?
?
PC
Wheat APPI +
SQ
SE
Impurity
TG
ST
1,3-DG
1,2-DG
?
ASG
MGDG
SG
GlcCer
DGDG
?
NAPE
?
?
PC
Yeast Corona
SQ
SE
Coenzyme Q6+TG
ST
FA
?
PG
PE
PA
PI
PC
Yeast APPI -
Impurity
Coenzyme Q6+TG
FA
?
?
PG
PE
PA
PI
PC
Yeast APPI +
SQ
SE
Impurity
Coenzyme Q6+TG
ST
?
PG
PE
PA
PI
PC
E. Coli Corona
Impurity
Coenzyme Q8
Impurity
PG
PE
CL
E. Coli APPI -
Impurity
Coenzyme Q8
PG
PE
CL
E. Coli APPI +
Impurity
Coenzyme Q8
PG
PE
CL

Figure 10. Chromatograms of 7 total lipid extracts, obtained by LC- Corona-CAD® (left), LC-APPI negative ion mode (middle) and LC-APPI positive ion mode (right). SQ-squalene, SE-sterol ester, CE-cholesteryl esters, TG-triacylglycerols, ST-sterols, Chol-cholesterol, DG-diacylglycerols, FA-fatty acids, MG-monoacylglycerols, ASG-acylated steryl glycosides, MGDG-monogalactosyldiglycerols, SG-steryl glycosides, GlcCer-glucosylceramides, HexCer-hexosylceramide, DGDG-digalactosyldiglycerols, NAPE-N-Acylphosphatidylethanolamines, PG-phosphatidylglycerols, PE-phosphatidylethanolamines, PA-phosphatidic acids, PI-phosphatidylinositols, CL-cardiolipins, PS-phosphatidylserines, PC-phosphatidylcholines, SM-sphingomyelins, LPC-lysophosphatidylcholines.